

2008

# Architecture and debugging of digital signal processing software in a high frequency MIL-STD-188-110A single tone receiver

Janette Marie Eberhard Provolt  
*Iowa State University*

Follow this and additional works at: <https://lib.dr.iastate.edu/etd>

 Part of the [Electrical and Computer Engineering Commons](#)

## Recommended Citation

Provolt, Janette Marie Eberhard, "Architecture and debugging of digital signal processing software in a high frequency MIL-STD-188-110A single tone receiver" (2008). *Graduate Theses and Dissertations*. 10873.  
<https://lib.dr.iastate.edu/etd/10873>

This Thesis is brought to you for free and open access by the Iowa State University Capstones, Theses and Dissertations at Iowa State University Digital Repository. It has been accepted for inclusion in Graduate Theses and Dissertations by an authorized administrator of Iowa State University Digital Repository. For more information, please contact [digirep@iastate.edu](mailto:digirep@iastate.edu).

**Architecture and debugging of digital signal processing software in  
a high frequency MIL-STD-188-110A single tone receiver**

by

Janette Marie Eberhard Provolt

A thesis submitted to the graduate faculty  
in partial fulfillment of the requirements for the degree of  
MASTER OF SCIENCE

Major: Electrical Engineering

Program of Study Committee:  
Zhengdao Wang, Major Professor  
Robert Weber  
Aleksandar Dogandzic

Iowa State University

Ames, Iowa

2008

Copyright © Janette Marie Eberhard Provolt, 2008. All rights reserved.

## DEDICATION

This thesis is dedicated to my wonderful husband, Brandon. Without his love, help and encouragement I would not have been able to complete this work. I am also dedicating this to my family and friends for their love, understanding and support throughout graduate school. Finally, this thesis is dedicated to my undergraduate professors Dr. Roger Green and the late Floyd Patterson for their guidance and encouragement to further my education, and for sparking my interest in signal processing.

## TABLE OF CONTENTS

<b>LIST OF FIGURES</b> . . . . .	v
<b>LIST OF TABLES</b> . . . . .	vii
<b>ABSTRACT</b> . . . . .	viii
<b>CHAPTER 1. INTRODUCTION</b> . . . . .	1
1.1 HF Communication Challenges . . . . .	1
1.2 HF Communication History . . . . .	5
1.3 Performance Requirements . . . . .	6
1.4 Organization of the Thesis . . . . .	8
<b>CHAPTER 2. MIL-STD-188-110A SINGLE-TONE MODEM</b> . . . . .	9
2.1 Over-the-air Specifications . . . . .	9
2.2 Top Level Transmit Data Processing . . . . .	12
<b>CHAPTER 3. CHANNEL MODEL AND RECEIVE PATH</b> . . . . .	19
3.1 Equivalent Channel Model . . . . .	21
3.2 Common Functionality . . . . .	22
3.3 Preamble Functionality . . . . .	24
3.3.1 Preamble Acquisition Mode . . . . .	25
3.3.2 Preamble Tracking Mode . . . . .	26
3.3.3 End of Preamble Mode . . . . .	28
3.4 Data/Probe Functionality . . . . .	28
3.4.1 Probe Correlators . . . . .	29
3.4.2 Channel Estimate . . . . .	32

3.4.3	Matched Filter, Equalizer, and Demodulator . . . . .	33
3.4.4	Deinterleaver, Decoder, and EOM Detector . . . . .	41
<b>CHAPTER 4. ISOLATION OF THE SOFTWARE DEFECT USING BIT</b>		
	<b>ERROR TIMING AND CHANNEL EFFECTS . . . . .</b>	<b>42</b>
4.1	Software Isolation using Bit Error Timing . . . . .	42
4.1.1	Errors at the Beginning of the Reception . . . . .	42
4.1.2	Errors at the End of the Reception . . . . .	46
4.1.3	Errors Throughout the Reception . . . . .	47
4.2	Software Isolation using Channel Effects . . . . .	48
4.2.1	Doppler Isolation . . . . .	49
4.2.2	Terminal Clock Difference Isolation . . . . .	52
4.2.3	Noise Isolation . . . . .	54
4.2.4	Frequency Dispersion Isolation . . . . .	57
4.2.5	Time Dispersion Isolation . . . . .	61
4.3	Software Isolation Summary . . . . .	68
<b>CHAPTER 5. SUMMARY AND FUTURE WORK . . . . .</b>		
<b>71</b>		
<b>APPENDIX</b>		
	<b>ACRONYMS . . . . .</b>	<b>73</b>
	<b>BIBLIOGRAPHY . . . . .</b>	<b>75</b>
	<b>ACKNOWLEDGEMENTS . . . . .</b>	<b>76</b>

## LIST OF FIGURES

Figure 1.1	Frequency Dispersion of 3 Hz . . . . .	3
Figure 1.2	Multipath . . . . .	4
Figure 1.3	Fading Caused by Time Dispersion . . . . .	4
Figure 2.1	Single Tone Over-the-Air Structure . . . . .	10
Figure 2.2	Detailed Transmit Block Diagram . . . . .	13
Figure 2.3	Interleaver Example . . . . .	14
Figure 2.4	Constellation Diagram of the Modulator Output . . . . .	15
Figure 2.5	Frequency Domain of the Waveshaper Output . . . . .	16
Figure 2.6	Frequency Domain of the Translator Output . . . . .	17
Figure 2.7	Quadrature Mix performed by the FPGA . . . . .	18
Figure 3.1	Receive Block Diagram . . . . .	19
Figure 3.2	HF Radio Receive Signal Processing Functionality . . . . .	20
Figure 3.3	Channel Model . . . . .	21
Figure 3.4	Single Tone Receive Common Functionality . . . . .	22
Figure 3.5	Receive Waveshaper Block Diagram . . . . .	23
Figure 3.6	Simplified Channel Model . . . . .	24
Figure 3.7	Single Tone Receive Preamble Functionality . . . . .	25
Figure 3.8	Single Tone Receive Data Functionality . . . . .	29
Figure 3.9	Probe Correlators . . . . .	30
Figure 3.10	Probe Correlation with 4 Sample Positions . . . . .	31
Figure 3.11	LMS Algorithm . . . . .	32

Figure 3.12	Matched Filter at the Receiver . . . . .	34
Figure 3.13	Matched Filter and Zero-Forcing Decision Feedback Equalizer . . . . .	35
Figure 4.1	Frequency Domain of the Translator Output with 0 and 70 Hz Doppler	50
Figure 4.2	Acquisition FFT Output with 0 and 70 Hz Doppler . . . . .	51
Figure 4.3	Original Probe Correlation and after Drift . . . . .	53
Figure 4.4	Equalized Constellation Diagram with 40 dB and 15 dB SNR . . . . .	56
Figure 4.5	Average Incoming Magnitude with 0 and 5 Hz of Frequency Dispersion	58
Figure 4.6	Average Incoming Magnitude and Corresponding Bit Errors with 5 Hz of Frequency Dispersion . . . . .	59
Figure 4.7	Average Incoming Magnitude and Corresponding Bit Errors with 0.5 Hz of Frequency Dispersion . . . . .	60
Figure 4.8	Probe Correlation with 0 msec and 5 msec of Time Dispersion . . . . .	62
Figure 4.9	Probe Correlation with 2 msec and 5 msec of Time Dispersion . . . . .	63
Figure 4.10	Probe Correlation with 5 dB and 0 dB Power Difference . . . . .	66
Figure 4.11	Unequalized and Equalized Constellation Diagrams with 2 msec of Time Dispersion . . . . .	67
Figure 4.12	Unequalized and Equalized Constellation Diagrams with 5 msec of Time Dispersion and 1 Hz of Frequency Dispersion . . . . .	68

## LIST OF TABLES

Table 1.1	Performance Requirements for Single Tone [3] . . . . .	7
Table 2.1	Data Rates, Interleaver Lengths, Encoding and Modulation Schemes for the Single Tone waveform . . . . .	10
Table 2.2	Preamble Field Length for Single Tone . . . . .	11
Table 2.3	Data and Probe Field Lengths for Single Tone . . . . .	11
Table 4.1	Preamble Sequence Example . . . . .	44
Table 4.2	Software Isolation based upon Bit Error Timing . . . . .	69
Table 4.3	Software Isolation based upon Individual Channel Effects . . . . .	70



## ABSTRACT

The MIL-STD-188-110A Single Tone high frequency modem is used by the United States military everyday as a beyond line-of-sight radio. Typically, beyond line-of-sight military radios use satellites for reflection. Satellite time is in high demand, and since there are a finite number of satellites in orbit, it makes over-the-air time expensive. The Single Tone high frequency modem offers a reliable alternative by using the ionosphere, rather than a satellite, for reflection. The ionosphere adds unique channel effects, causing the signal processing software to be more complex and harder to debug than radios which use satellites.

Before being placed into production, the MIL-STD-188-110A Single Tone high frequency modem is placed under comprehensive performance tests. These tests are meant to fully verify all aspects of the software and to impose all possible channel effects such as additive white Gaussian noise, doppler shift, terminal clock differences, frequency and time dispersion. When a test fails, debugging the software can be tedious and time consuming. The two major steps to quick and successful debugging are understanding and isolation. The engineer must understand the channel model and receive path in order to correlate a test failure with a specific section of software. After the channel model and receive path are understood, timing patterns of bit errors and test failures caused by individual channel effects help the engineer isolate the software defect. This thesis compiles the necessary information to understand a generalized receive path and provides a framework for isolating a software defect.

## CHAPTER 1. INTRODUCTION

There are many types of over-the-air communications used by the United States military today, and many are able to transmit beyond line-of-sight (LOS), but most require the use of a satellite for reflection. Since satellites are expensive to launch and maintain, there are a finite number of satellites in orbit, which makes satellite time high in demand and expensive to use. High frequency (HF) offers an alternative for beyond LOS communication. HF uses frequencies between 3 MHz and 30 MHz and relies on the earth's ionosphere for reflection, making beyond LOS communication possible without the use of a satellite.

Some typical challenges associated with over-the-air communication include noise, doppler shift, and terminal clock differences. HF communication also encounters challenges associated specifically with the use of the ionosphere. According to Furman and Nieto, "The HF channel is characterized as a multi-path time-varying environment that produces time and frequency dispersion." [6]. Frequency and time dispersion add to the complexity of the signal processing in HF radios. With the added complexity, it can be very difficult to isolate issues seen during performance testing. This thesis provides a matrix of information to help isolate a software defect.

### 1.1 HF Communication Challenges

Noise, doppler shift, and terminal clock differences occur with every over-the-air transmission, regardless of whether or not the ionosphere is used for reflection. Noise occurs over any channel and can be thought of as a source of an additive random signal. In most cases, the noise is assumed to be additive white Gaussian noise (AWGN). Many waveforms require a minimum signal-to-noise ratio (SNR) to acknowledge a signal. If the noise power is too high

with respect to the signal power, the minimum SNR is not met and the receiving terminal does not detect the signal.

Doppler shift is caused by the relative movement of either the transmitting or receiving terminal. It causes the receiving terminal to detect a signal that is shifted in frequency from the expected carrier. Many waveforms have a maximum doppler shift setting for which they correct. If the doppler shift detected is greater than this limit, the receiving terminal corrects for the maximum doppler shift and some amount of uncorrected frequency offset remains in the signal. This causes bit errors or a potential loss of signal.

Timing differences between the transmitting and receiving terminals are caused by the internal clocks. If the clock on the transmitting terminal is faster or slower than the clock on the receiving terminal, the receiving terminal slowly sees the received signal drift. If not addressed by the receiver, this eventually causes bit errors and a loss of signal.

Frequency and time dispersion occur with communications which use the ionosphere for reflection. Ionospheric fading occurs when the ionosphere absorbs signal energy during transmission. The ionosphere absorbs signal energy at different rates, depending on the density of the ionosphere. According to Nieto, since the density of the ionosphere is not constant or predictable, it is impossible to find a “fixed relationship between distance and signal strength for ionospheric propagation” [1]. Since the rate at which energy is absorbed is not constant, it causes frequency dispersion. The top image in Figure 1.1 shows the average incoming amplitude with no frequency dispersion, and the bottom image shows the effects of frequency dispersion.

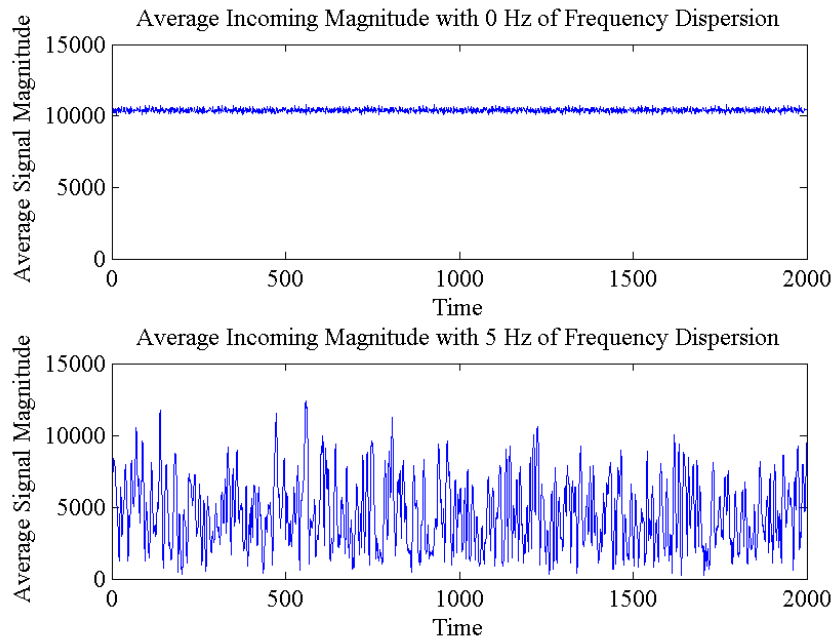


Figure 1.1 Frequency Dispersion of 3 Hz

Time dispersion occurs when a signal takes multiple paths to the receiving terminal, as seen in Figure 1.2. According to Furman and Nieto, “the sources of multi-path are the reflections of radio signals from different layers in the ionosphere. In addition, multiple reflections can occur between the earth’s surface and the ionosphere” [6]. These multiple paths cause the received signal to contain “several ‘echoes’ or modes, separated in time by a matter of milliseconds” [6]. This makes it difficult for the receiver to decipher the signal.

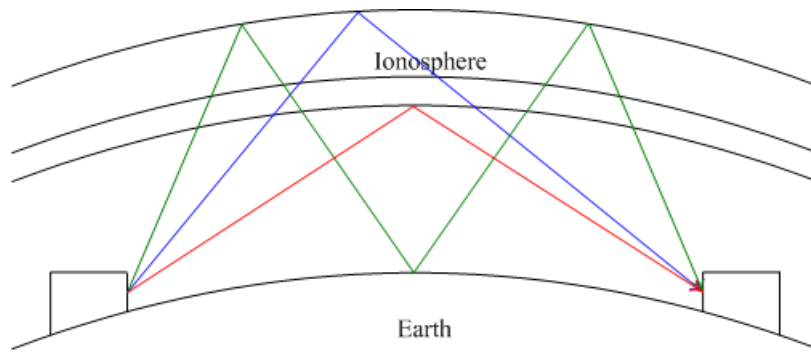


Figure 1.2 Multipath

In addition to overlapping, these signals destructively interfere as shown in Figure 1.3. This interference appears to the receiving terminal as a single signal with fading.

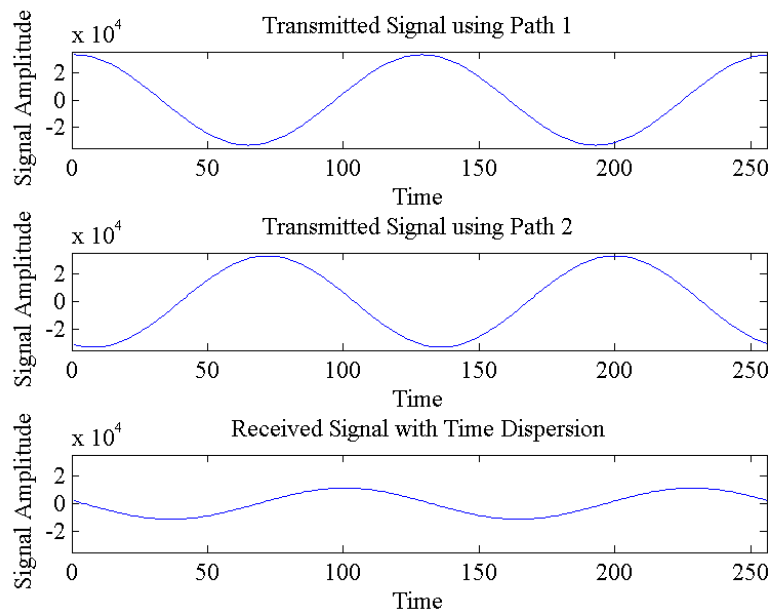


Figure 1.3 Fading Caused by Time Dispersion

The two largest issues with HF communication are the effects of frequency and time dispersion. Since neither frequency nor time dispersion can be prevented, methods were introduced

into the military standards to minimize their effect.

The following are possible ways to approach the time dispersion issue [1]:

- Adaptive Equalization
- Maximum Likelihood Sequence Elimination
- Guard-time protection

The following are ways of approaching the frequency dispersion issue [1]:

- Frequency Diversity
- Time Diversity
- Antenna Diversity
- Bandwidth Expansion
- Coding and Interleaving

To minimize the effects of frequency and time dispersion, the military standards for HF communications have evolved over time to incorporate the items listed above.

## 1.2 HF Communication History

Military standards were created by the government to ensure commonality, compatibility and reliability between military radios. They define the structure of communication and set performance standards. One of the first restrictions limited the bandwidth to 3 kHz. This maximized the number of communications that could occur over the HF frequency band. Unfortunately, limiting the bandwidth to 3 kHz also introduced the effects of inter-symbol interference (ISI) for digital communication.

In the early stages of HF communication, the continuous wave (CW) and amplitude modulation (AM) were the most common standards for HF communication. Unfortunately, efficiency of CW is limited to the efficiency of the user's knowledge of Morse code. AM was popular

because the implementation simplicity is comparable to CW, and it has the advantage that the user does not have to be familiar with Morse code. The disadvantage to AM is the bandwidth inefficiency. According to the HF Communications Data Book, the AM waveform “occupies a wide spectrum and is inefficient in the sense that a great deal of unneeded carrier (5 kHz) is generated to carry the modulation” [2]. To eliminate this inefficiency, single sideband (SSB) waveforms were created. A SSB waveform carries the same amount of information as a double sideband (DSB) waveform, but only transmits the upper sideband (USB) or lower sideband (LSB), greatly reducing the needed bandwidth. One of the first standardized waveforms to use the SSB idea was the frequency shift keying (FSK) waveform described in MIL-STD-188-110B.

Even though SSB FSK is more efficient than the previous methods, it still battles reliability issues caused by frequency and time dispersion. According to the HF Communications Data Book, “spatial diversity and frequency diversity were commonly used to improve the reliability. However, due to bandwidth and resource limitations,” [2] another standardized waveform, Single Tone, was introduced and can be found in MIL-STD-188-110A. The Single Tone waveform still uses SSB for bandwidth efficiency, but instead of using spatial and frequency diversity to battle frequency and time dispersion as FSK does, it uses encoding, interleaving, and equalization. Single Tone will be the HF waveform focus for the remainder of this thesis.

### 1.3 Performance Requirements

Interoperability is ensured in all military radios through the use of military standards. The Single Tone modem performance standard requires that a receiver must be able to detect and correct for a maximum doppler shift of 75 Hz [3]. There is not a specific performance requirement pertaining to terminal clock differences, but the modem must implement a mechanism to correct for clock differences in order to communicate with other radios for several consecutive hours.

In addition to doppler shift, the military standard also sets requirements for noise, frequency and time dispersion and can be seen in Table 1.1. These standards require that a minimum

bit error rate (BER) be met under certain channel conditions. The military standards use the Watterson model as a channel simulator and a way to standardize the BER performance.

Table 1.1 Performance Requirements for Single Tone [3]

Data Rate	Interleaver	Time Delay	Frequency Spread	SNR	Required BER
4800	None	N/A	N/A	17 dB	0.001
4800	None	2 msec	0.5 Hz	27 dB	0.001
2400	Long	N/A	N/A	10 dB	0.00001
2400	Long	2 msec	1 Hz	18 dB	0.00001
2400	Long	2 msec	5 Hz	30 dB	0.00001
2400	Long	5 msec	1 Hz	30 dB	0.00001
1200	Long	2 msec	1 Hz	11 dB	0.00001
600	Long	2 msec	1 Hz	7 dB	0.00001
300	Long	5 msec	5 Hz	7 dB	0.00001
150	Long	5 msec	5 Hz	5 dB	0.00001
75	Long	5 msec	5 Hz	2 dB	0.00001

Noise is represented in the table through SNR. The lower SNR contains higher noise levels with respect to the signal level. When describing the HF channel, according to Furman and Nieto, “The amount of multi-path can range up to 6 msec and the fading rate can be as high as 5 Hz” [6]. If time dispersion is required, it is represented in the table by the arrival time difference between the first and second signal and is measured in milliseconds. The number of paths is fixed at two and the power of each signal is equal. Frequency dispersion is represented as the rate at which the average signal amplitude changes, and is measured in Hz. With respect to frequency dispersion in channel simulators, the maximum and minimum amplitudes of the signal are predetermined, but the frequency at which it changes is modifiable.

While performance testing, it can be difficult to isolate the signal processing software to debug the problem. As described above, there are many challenges incorporated into the HF channel including noise, doppler shift, terminal clock differences, frequency and time dispersion. This thesis explores debugging methods that can be used to solve test failures. The two major steps to successful debugging are understanding and isolation. The engineer must understand the channel model and receive path in order to correlate a test failure with a specific section of



software. After the channel model and receive path are understood, the isolation of a software defect through timing patterns of bit errors and individual channel effects is possible.

## 1.4 Organization of the Thesis

This thesis is organized in the following manner.

- Chapter 1 explains why HF communications are used and the challenges associated with the HF channel. It also describes how the military standards have evolved over time to minimize some of these challenges. Performance requirements, set by the military standard, are also discussed.
- Chapter 2 presents the over-the-air specifications for the Single Tone HF waveform. Also discussed is a high level overview of the transmit data processing.
- Chapter 3 explains the channel model and the entire receive path.
- Chapter 4 explains methods of isolating a software defect through timing patterns of bit errors and individual channel effects.
- Chapter 5 summarizes the thesis and suggests future work.

## CHAPTER 2. MIL-STD-188-110A SINGLE-TONE MODEM

There are many different types of signal processing the HF waveform uses to communicate signals over-the-air. Each type of processing produces a unique waveform, as described in their respective military standards. This chapter contains an overview of the over-the-air specifications for the Single Tone HF waveform, as described in MIL-STD-188-110A [3]. Also discussed is a high level overview of the transmit data processing.

### 2.1 Over-the-air Specifications

The Single Tone waveform converts binary information into a single M-ary phase shift keying (PSK) modulated output carrier and is described in MIL-STD-188-110A [3]. The possible data rates defined for the Single Tone waveform are 75, 150, 300, 600, 1200, 2400, and 4800 bits per second (bps). A forward error correction (FEC) encoding rate of  $\frac{1}{2}$  is used along with an interleaver to minimize bit errors. The possible interleaver lengths are 0.6 and 4.8 seconds. Since interleaving comes before modulation, the length of the interleaver (in bits) varies, depending on the data rate. See table 2.1 for a complete list of possible combinations of data rates, interleaver lengths, encoding and modulation schemes.

Figure 2.1 illustrates the structure of a Single Tone transmission. The major components within the transmission structure are preamble, data and probe blocks. Contained within the last data blocks are the EOM and flush.

Table 2.1 Data Rates, Interleaver Lengths, Encoding and Modulation Schemes for the Single Tone waveform

Data Rate	Interleaver	FEC Encoding	Data Modulation
75 bps	0.6 or 4.8 sec	$\frac{1}{2}$	Multiple PSK symbols per channel symbol
150 bps	0.6 or 4.8 sec	$\frac{1}{2}$	2-ary PSK scrambled to appear 8-ary
300 bps	0.6 or 4.8 sec	$\frac{1}{2}$	2-ary PSK scrambled to appear 8-ary
600 bps	0.6 or 4.8 sec	$\frac{1}{2}$	2-ary PSK scrambled to appear 8-ary
1200 bps	0.6 or 4.8 sec	$\frac{1}{2}$	4-ary PSK scrambled to appear 8-ary
2400 bps	0.6 or 4.8 sec	$\frac{1}{2}$	8-ary PSK scrambled to appear 8-ary
4800 bps	0 sec	None	8-ary PSK scrambled to appear 8-ary

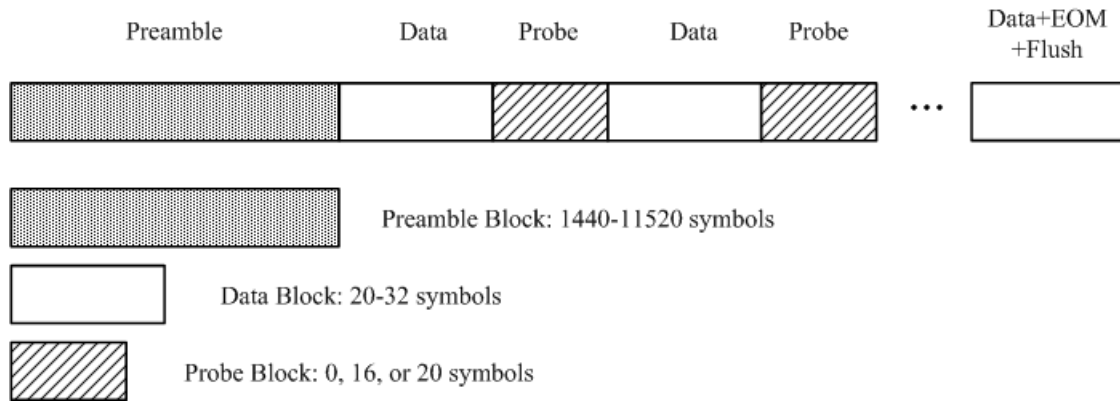


Figure 2.1 Single Tone Over-the-Air Structure

From the Single Tone transmission structure, there are four different states important for transmission and reception:

- *Variable Length Preamble* – At the receiver, the preamble is used for initial synchronization, relative motion doppler estimation, and automatically determining the transmitted data rate and interleaver length (autobaud). The process of autobaud does not require the modem to have prior knowledge of the transmitted data rate or interleaver length. The preamble occurs at the very beginning of the transmission and is made of segments, each 200 msec long. The interleaver length determines the number of segments transmitted for the preamble, as shown in table 2.2.

Table 2.2 Preamble Field Length for Single Tone

Interleaver Length	Preamble Field Length
0.6 sec	3 segments
4.8 sec	24 segments

For an interleaver length of 0.6 seconds, the preamble contains 3 segments, and 24 segments for the 4.8 second interleaver. For each segment, there are 15 elements, each ranging from 0 to 7. All 8 possible elements are mapped to a unique 32 bit pattern for transmission. The receiver uses two elements within a segment to determine the auto-baud information and three to determine the preamble count. The remaining elements are used for synchronization.

- *Variable Length Data And Probe* – This portion contains alternating data (unknown) and probe (known) fields. The probe provides the receiver with a set of known symbols. The receiver uses these symbols to calculate a channel estimate to be used for equalization. The probes are also used to monitor relative motion doppler and timing differences between the transmitting and receiving radio clocks and to detect if time dispersion exists. The number of symbols in each field is dependent on the selected data rate, as shown in table 2.3.

Table 2.3 Data and Probe Field Lengths for Single Tone

Data Rate	Data Field Length	Probe Field Length
4800 bps	32 symbols	16 symbols
2400 bps	32 symbols	16 symbols
1200 bps	20 symbols	20 symbols
600 bps	20 symbols	20 symbols
300 bps	20 symbols	20 symbols
150 bps	20 symbols	20 symbols
75 bps	32 symbols	0 symbols

Notice that at 75 bps, probe fields are not used. The 75 bps rate is handled differently

by the Single Tone modem and many times is considered a separate waveform. The remainder of this thesis handles data rates 150 to 4800 bps, where probe fields are used.

- *End of Message (EOM)* – The end of message is embedded within the data field and is a specific sequence that the receiving modem uses to detect the end of the current message. Once detected at the output of the decoder, the modem knows it is the end of the current reception and begins looking for the preamble of a new message.
- *Flush Bits* – The flush bits are all zeros and are contained within the data field. These bits are used on both the transmitter and receiver to flush valid data and the EOM through the encoder/decoder and interleaver/deinterleaver.

## 2.2 Top Level Transmit Data Processing

The signal processing code, or the modem, transitions through the four states, as described in section 2.1, as soon as it begins receiving bits for transmission. The modem executes the first state by sending the defined preamble. Once the entire preamble is sent, the transmit modem transitions to the second state. While in the second state, the modem sends alternating data and probe pairs, where the probe sections are known symbols and the data sections are symbols translated from the incoming bits. Once the end of data is detected, the transmit modem transitions to the third and fourth state, sending the EOM and flush bits, respectively.

The detailed transmit block diagram for data flow, including preamble, data and probes, is shown in figure 2.2. In order for the signal processing code to convert bits into complex samples to be sent to the exciter, the bits pass through an encoder, interleaver, modulator, waveshaper, translator, and a rate change filter.

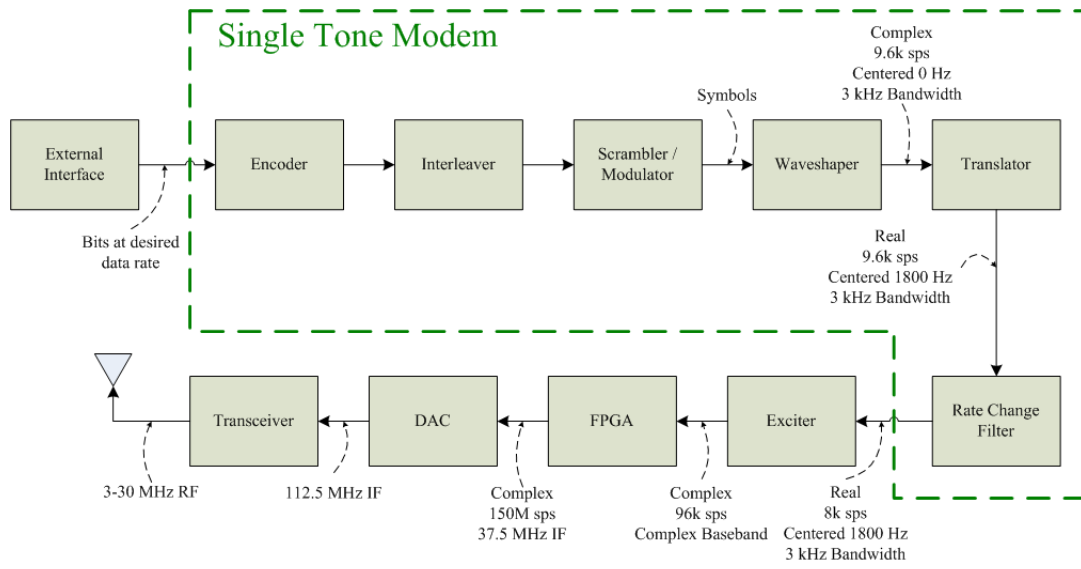


Figure 2.2 Detailed Transmit Block Diagram

An encoder is used to limit errors in the data reception by adding redundant bits to the transmission. The redundant bits allow the decoder to have a better chance of correctly decoding the data, even if there are bit errors scattered throughout the received signal. In Single Tone, the encoder uses  $\frac{1}{2}$  FEC encoding with 7 taps to encode the bits. This encoding scheme doubles the original amount of data to be inserted into the interleaver.

The interleaver is used to scramble the data to avoid burst errors and to combat frequency dispersion. Figure 2.3 illustrates how burst errors are scattered at a receiver. Once scattered, the redundant bits created by the encoder allow the Viterbi decoder to have a better chance of correctly decoding the bits. Typically, interleavers are created from a matrix of columns and rows. The incoming data is placed into the columns in a specific order. Once the interleaver is full, it is unloaded by rows. In channels which contain only AWGN, interleavers have no advantage since bit errors occur randomly throughout the channel. However, in HF communications, frequency and time dispersion cause burst errors which are dispersed by the interleaver.

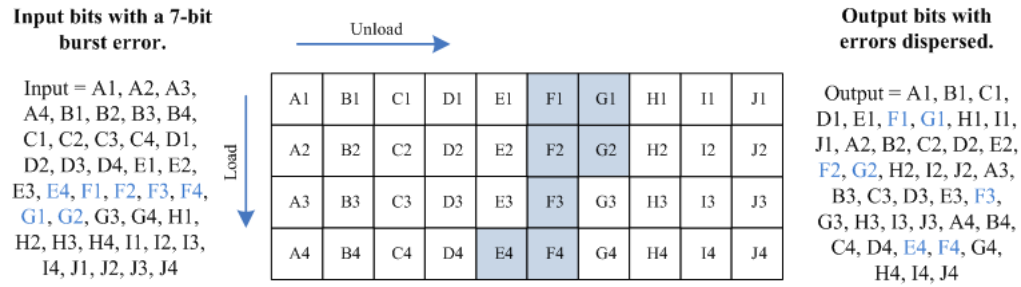


Figure 2.3 Interleaver Example

Next, the encoded and interleaved data pass through a modulator. The modulator uses gray encoding to help maximize error recovery at the receiver by ensuring the adjacent symbols around the unit circle differ by only one bit. If the receive modem chooses a symbol incorrectly by choosing the neighboring symbol, the result contains only one bit error. The modulator maps the bits into complex symbols which have a constant rate of 2400 symbols per second (sps). Figure 2.4 shows the 8-ary PSK constellation diagram for a Single Tone transmission, created by using a data rate of 2400 bps.

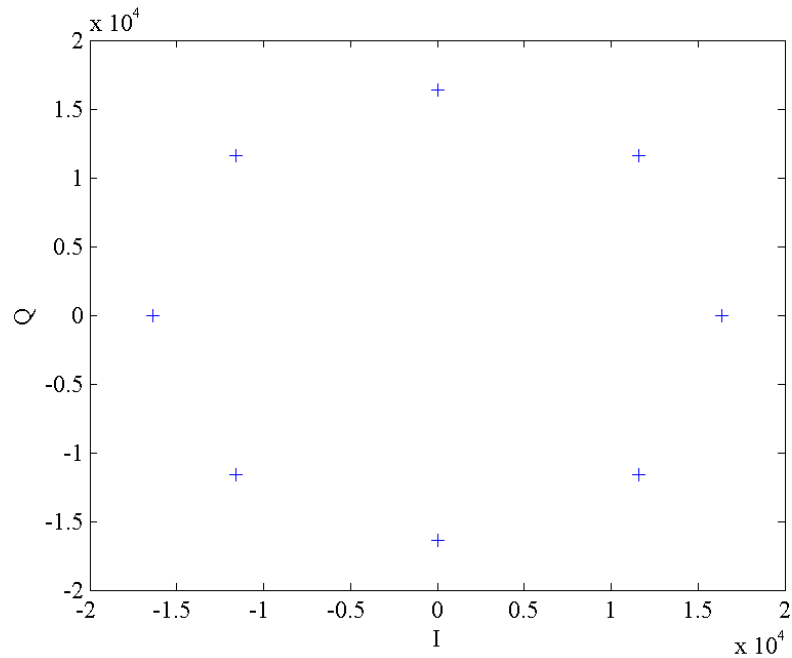


Figure 2.4 Constellation Diagram of the Modulator Output

After modulation, the data is passed through a waveshaper, where a low pass filter is applied to the symbols. Since HF is band-limited to 3 kHz, the waveshaper limits the bandwidth of the signal. The waveshaper also performs a 4 to 1 up-sampling, bringing the output symbol rate up to 9600 sps. Figure 2.5 shows the frequency domain of the waveshaper output. Notice the signal is centered at 0 Hz, and has a bandwidth of roughly 3 kHz.



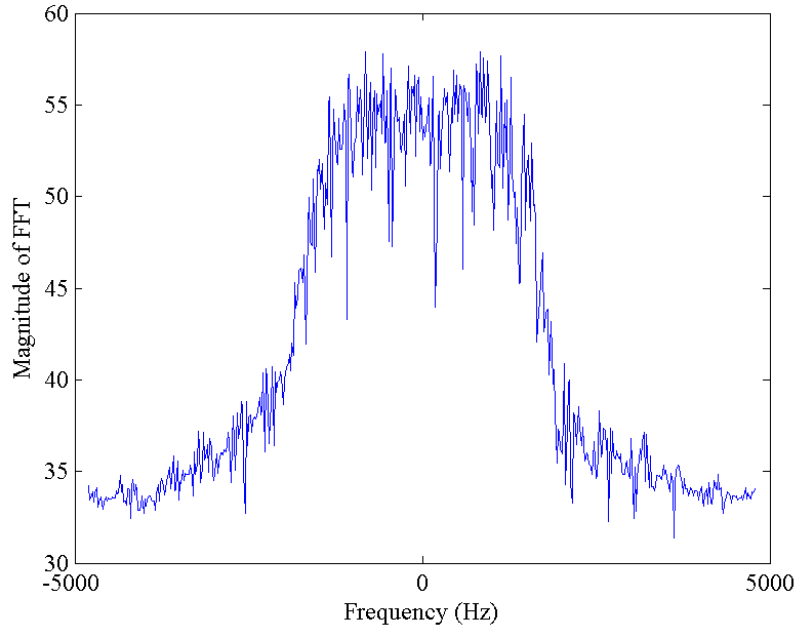


Figure 2.5 Frequency Domain of the Waveshaper Output

Let  $v[n]$  represent the output of the waveshaper. Then,

$$v[n] = \sum_{k=0}^{\infty} I[k]g[n - k] \quad (2.1)$$

where  $I[n]$  represents the symbols created from the modulator and  $g[n]$  represents the waveshaper. As discussed previously, band-limitation causes ISI. To minimize the effects of ISI, a square root raised cosine is used as the low pass filter instead of a sinc function and is given below.

$$g[n] = \frac{2\beta}{\pi\sqrt{T_s}} \frac{\cos\left[(1+\beta)\pi\frac{n}{T_s}\right] + \frac{\sin\left[(1-\beta)\pi\frac{n}{T_s}\right]}{4\beta\frac{n}{T_s}}}{\left[1 - \left(4\beta\frac{n}{T_s}\right)^2\right]} [7]$$

Where  $T_s$  is the symbol period and  $\beta$  is the configurable roll-off factor. The square root raised cosine was specifically chosen for reducing ISI, since the zero crossings in the time domain occur at multiples of the symbol rate, or every  $T_s$  seconds [7].

After waveshaping, the data is passed through a translator. The translator uses a complex oscillator to shift the center frequency of the incoming signal to a +1800 Hz sub-carrier. The equation used to shift  $v[n]$  to the +1800 Hz sub-carrier is shown in equation 2.2. Let  $s[n]$  be the output of the translator and  $v[n]$  is the output of the waveshaper.

$$\begin{aligned} s[n] &= \text{Re}\{v[n][\cos(1800n) + j \sin(1800n)]\} \\ &= \text{Re}\{v[n]e^{j2\pi 1800n}\} \end{aligned} \quad (2.2)$$

The translator shifts the signal by +1800 Hz and converts it into a real signal. Figure 2.6 shows the frequency domain of the translator output. Now the 3 kHz signal is centered at +1800 Hz.

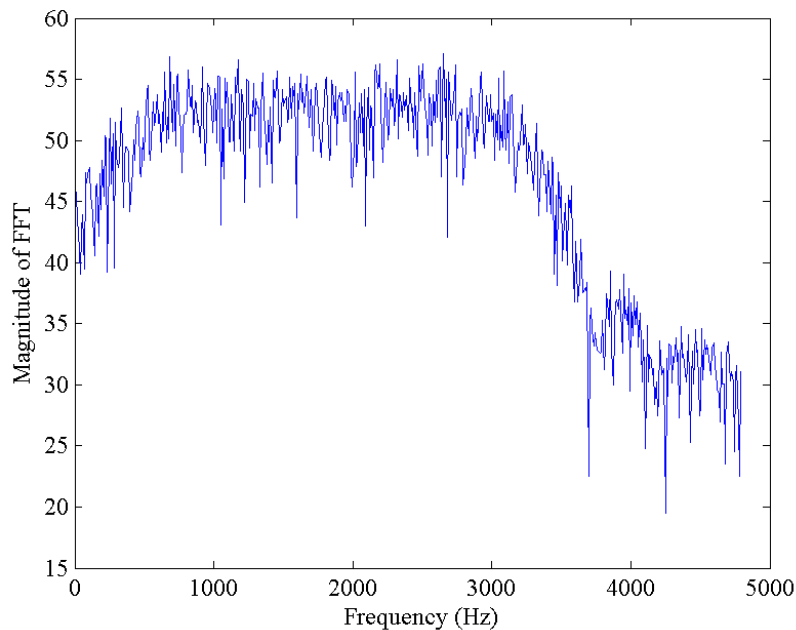


Figure 2.6 Frequency Domain of the Translator Output

The 9.6k sps real signal is passed through a rate change filter after translation. The purpose of the rate change filter is to decimate the 9.6k sps signal to an 8k sps signal. This filter was designed to bridge the gap between a legacy modem and the exciter. The rate change filter

is implemented as a polyphase filter which interpolates the 9.6k sps signal to 96k sps, then decimates to 8k sps. The output of the rate change filter is a real 8k sps audio signal.

The rate change filter is the final block of the Single Tone modem software. The exciter, field programmable gate array (FPGA), digital to analog converter (DAC), and transceiver implement additional signal processing functions needed for an HF radio. The exciter has three major responsibilities: complex bandpass filtering, LSB/USB selection, and interpolation. The incoming real 8k sps audio signal is first passed through a complex bandpass filter. If LSB, rather than USB, is desired, the exciter will invert the center frequency of the signal from 1800 to -1800 Hz. The exciter then interpolates the complex signal from 8k sps to 96k sps before passing it to the FPGA. The FPGA uses a quadrature mixer to translate and interpolate the complex 96k sps baseband signal to a complex 150M sps signal at an intermediate frequency (IF) of 37.5 MHz. Figure 2.7 shows an image of the signal centered at  $\pm 37.5$  MHz, and the aliased signal located at  $\pm 112.5$  MHz.

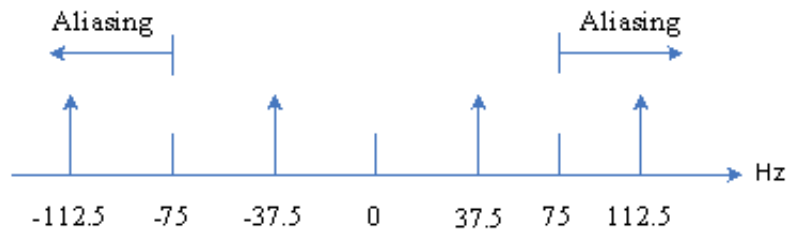


Figure 2.7 Quadrature Mix performed by the FPGA

The complex 150M sps signal centered at 37.5 MHz is passed from the FPGA to the DAC. Instead of using the signal located at 37.5 MHz, the DAC uses the aliased signal at 112.5 MHz and converts it to analog. The analog signal, centered at 112.5 MHz, is passed to the transceiver where the signal is translated a radio frequency (RF) ranging from 3 to 30 MHz. The resulting analog signal at RF is ready for over-the-air transmission.

### CHAPTER 3. CHANNEL MODEL AND RECEIVE PATH

The first step in debugging problems encountered during performance testing is understanding the receive path and channel. Without this understanding it is difficult to isolate the target software to debug, even after the channel effect causing the issue is known. A block diagram of the entire receive path can be seen in Figure 3.1. In the figure, there are four major blocks including the HF radio receive signal processing functionality, Single Tone receive common, preamble and data/probe functionality.

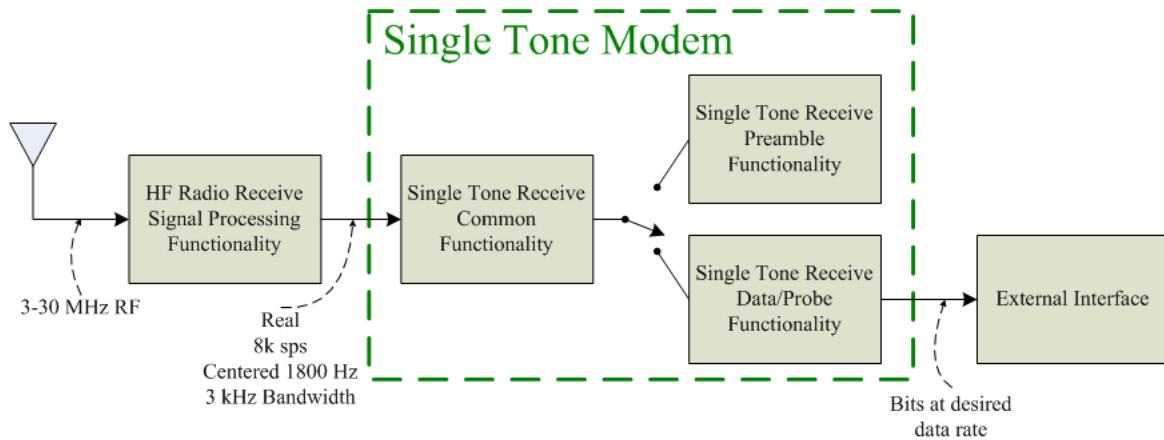


Figure 3.1 Receive Block Diagram

As discussed in section 2.2, the exciter, FPGA, analog to digital converter (ADC), and transceiver are four major components that are not a part of the Single Tone modem, but contain important functionality for HF radios. These components can be seen as part of the HF radio receive signal processing functionality in Figure 3.1, and can be seen in detail in Figure 3.2.

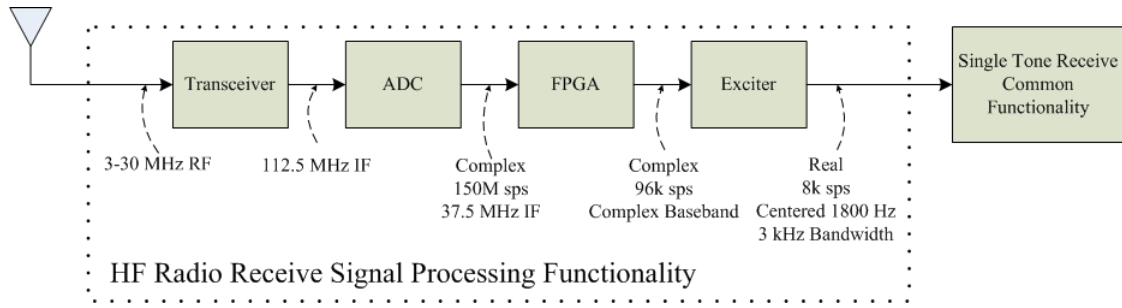


Figure 3.2 HF Radio Receive Signal Processing Functionality

The analog RF signal, ranging from 3 to 30 MHz, is sent into the transceiver where the signal is translated to an IF frequency of 112.5 MHz. The ADC converts the analog signal to a complex digital signal centered at 37.5 MHz IF with a sample rate of 150M sps. The FPGA uses a quadrature mixer to translate and decimate the complex 150M sps signal at 37.5 MHz IF to a 96k sps baseband signal. Next, the exciter decimates the 96k sps complex baseband signal to an 8k sps real signal. It also translates the signal from -1800 to 1800 Hz, if LSB was used, before passing it to the Single Tone receive common functionality.

The remainder of this thesis focuses on the Single Tone receive common, preamble and data/probe functionality in addition to the equivalent channel model. As discussed in section 2.1, the Single Tone waveform has four states including the preamble, data and probe pairs, EOM and flush. Upon reception, all received samples proceed through common functionality. After the common functionality, the symbols take different receive paths based on whether or not the preamble has been received. Initially, the received samples travel the preamble path until it is determined the entire preamble is received at which point the samples switch to the data path. The data path is responsible for the data/probe pairs along with the EOM and flush.

The channel model includes three major transmit blocks that have been previously discussed including the modulator, waveshaper and translator. Also included in the channel model is AWGN and channel effects such as frequency and time dispersion.

### 3.1 Equivalent Channel Model

The channel model is shown below in Figure 3.3. There are three major blocks included in Figure 3.3 that are important to the architecture and have been previously discussed in section 2.1. The modulator takes encoded and interleaved bits and maps them to symbols,  $I[n]$ , depending on the type of modulation. To band-limit the transmitted signal, the symbols are placed through a low-pass filter with total bandwidth of 3 kHz, also known as the waveshaper. A square root raised-cosine,  $g[n]$ , is used to implement the low-pass filter to minimize the effects of inter-symbol interference. After waveshaping, the signal is then translated from 0 to 1800 Hz. The outputs of the waveshaper and translator are represented by  $v[n]$  and  $s[n]$  in Figure 3.3.

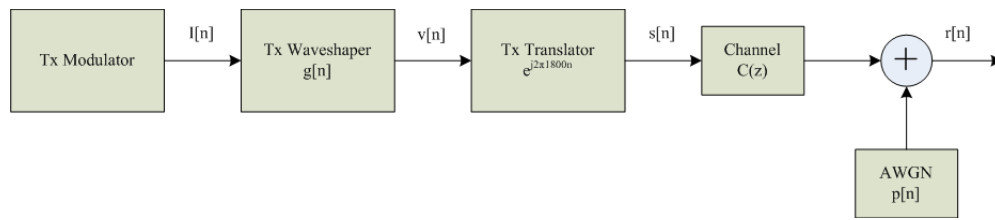


Figure 3.3 Channel Model

The output of the waveshaper,  $v[n]$ , was defined in Equation 2.1 and is shown below.

$$v[n] = \sum_{k=0}^{\infty} I[k]g[n - k]$$

The frequency shift of the translator is represented in Figure 3.3 by  $e^{j2\pi 1800n}$  and the resulting output,  $s[n]$ , was defined in Equation 2.2 and is shown below.

$$s[n] = \text{Re}\{v[n]e^{j2\pi 1800n}\}$$

In Figure 3.3, the channel effects such as doppler shift, terminal clock differences, frequency and time dispersion, are represented by  $c[n]$  or  $C(z)$ . AWGN is also added and is represented by  $p[n]$ . The received signal can be represented in the frequency domain by,

$$R(z) = S(z)C(z) + P(z)$$

or in the time domain,

$$\begin{aligned} r[n] &= s[n] \otimes c[n] + p[n] \\ &= \sum_{k=-\infty}^{\infty} s[k]c[n - k] + p[n] \end{aligned}$$

Where  $\otimes$  represents the convolution of two signals.

### 3.2 Common Functionality

As shown in Figure 3.4, the received signal,  $r[n]$ , passes through some Single Tone receive common functionality, regardless of whether it is the preamble, data and probe pairs, EOM or flush. The common functionality block diagram is shown in detail in Figure 3.4.

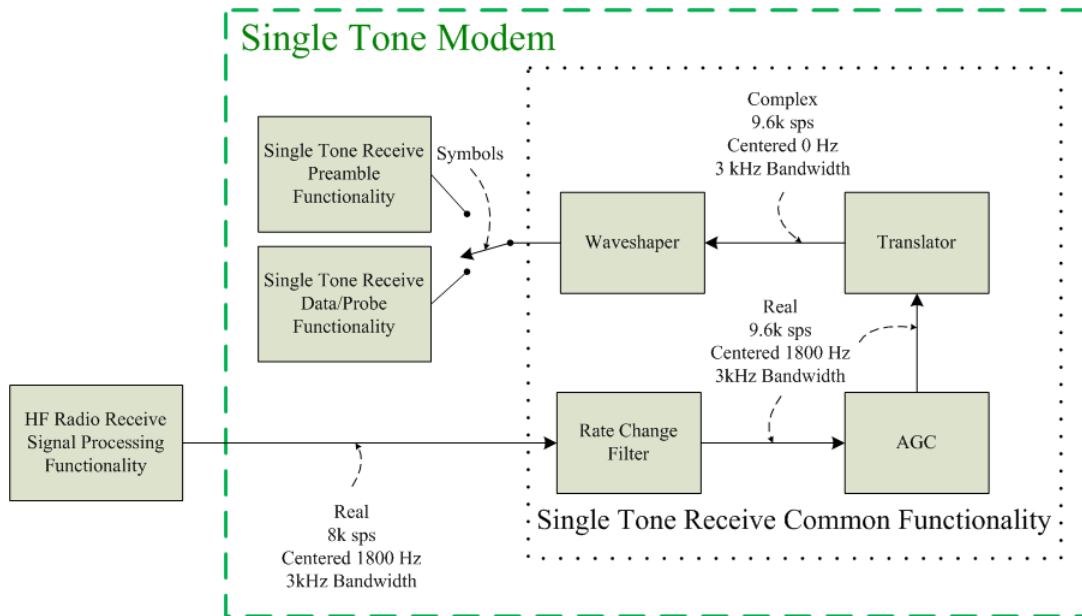


Figure 3.4 Single Tone Receive Common Functionality

The first block in the diagram is the rate change filter. Similar to the transmit logic, the rate change filter is used as an interface between two pieces of legacy code. The polyphase

filter interpolates the 8k real signal to 96k sps before decimating down to 9.6k sps. The output of the rate change filter is then passed to the automatic gain control (AGC).

The AGC is a control loop which uses the output signal level strength to vary the gain on the input signal. It smoothes the amplitude envelope to avoid drastic changes in signal level, and maximizes dynamic range. After the AGC, the received signal is shifted by the translator.

Similar to the transmit functionality, a complex oscillator is used to translate the real signal at 1800 Hz to a complex signal at 0 Hz. The 3 kHz bandwidth of the signal remains unchanged. The output of the translator is then passed to the waveshaper.

The waveshaper uses a transversal filter to decimate the signal by four and negate the effects of the pulse shaping, placed on the signal at the transmitter. A block diagram of the waveshaper can be seen in Figure 3.5. The receive waveshaper down-samples the 9600 sps signal by four at each of the four sample timing positions, resulting in four signals at 2400 symbols per second. The down-sampling at each timing position is done to allow the receive path to determine and use the timing position which closest resembles the transmitted signal.

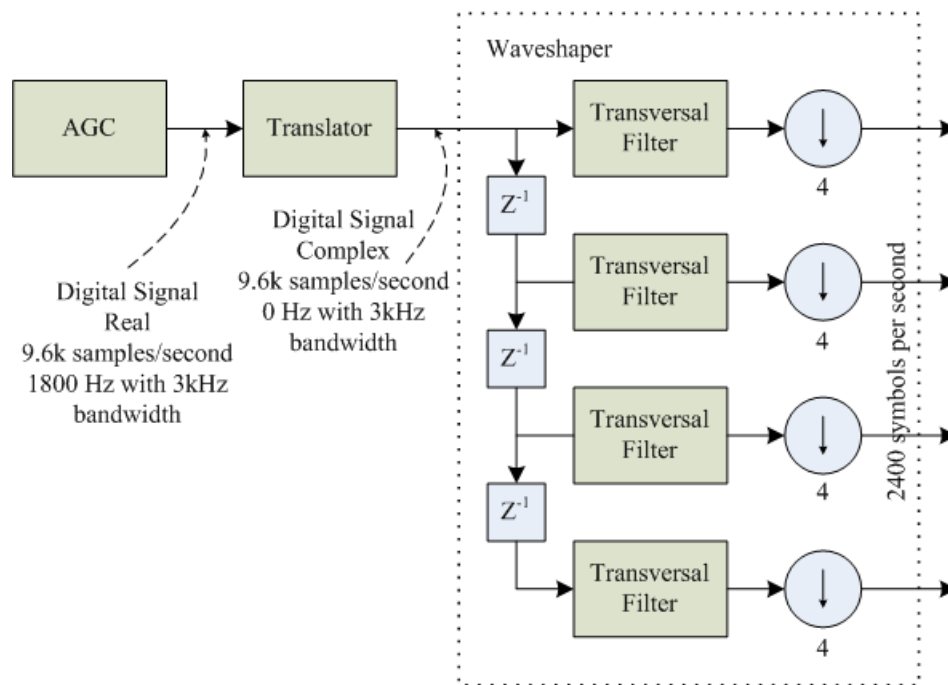


Figure 3.5 Receive Waveshaper Block Diagram



To simplify the channel model, the effects of the rate change filter, AGC, translator, and waveshaper are filtered into the channel effects and a simplified model is shown below in Figure 3.6. The new channel and noise models are  $H(z)$  and  $z[n]$ , respectively, and the new received signal,  $r_w[n]$ , now represents the output of the receive waveshaper.

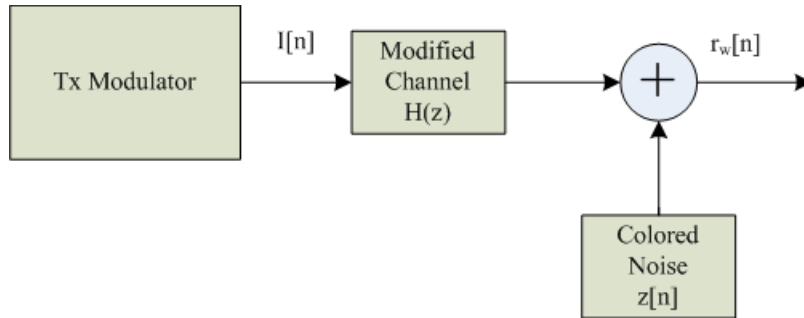


Figure 3.6 Simplified Channel Model

The equivalent received signal can be represented in the frequency domain by,

$$R_w(z) = I(z)H(z) + Z(z)$$

or in the time domain,

$$r_w[n] = I[n] \otimes h[n] + z[n] \quad (3.1)$$

$$= \sum_{k=-\infty}^{\infty} I[k]h[n-k] + z[n] \quad (3.2)$$

### 3.3 Preamble Functionality

After the waveshaper, the received signal enters into the Single Tone receive preamble functionality unless a preamble has previously been received. There are three modes of the preamble path including acquisition, tracking and end of preamble. A block diagram of the preamble path is shown in Figure 3.7.

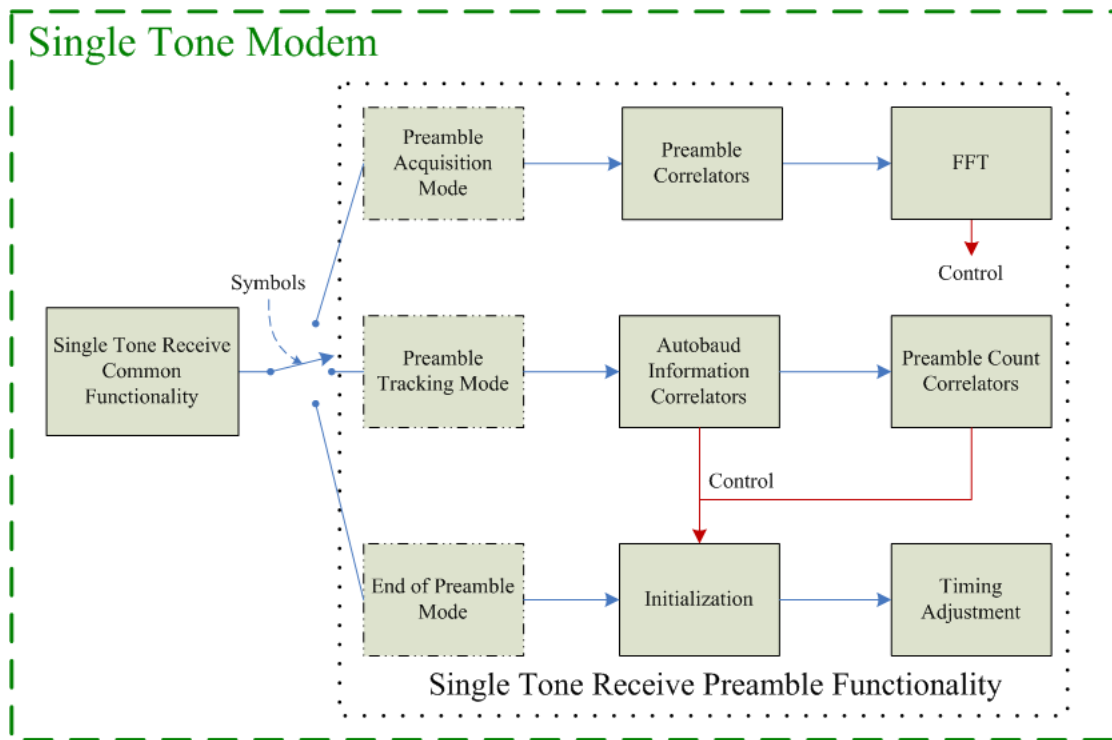


Figure 3.7 Single Tone Receive Preamble Functionality

### 3.3.1 Preamble Acquisition Mode

The purpose of the preamble acquisition mode is to determine the beginning of the preamble. To do this, the terminal correlates the incoming signal with a section of the known preamble sequence. The correlation is then placed through a fast Fourier transform (FFT) to determine a noise to signal ratio (NSR). In order to declare a signal present, the NSR must be less than a pre-defined threshold. Once it is determined that a signal is present, the current preamble timing position is calculated based upon the index of the maximum correlation peak, and the initial doppler offset calculated from the FFT output is fed back into the translator. The translator uses this data to alter the frequency translation. Instead of translating by 1800 Hz, the translator shifts the signal 1800 Hz plus the initial doppler offset.

To ensure the FFT will account for a 75 Hz doppler shift, the precision of the FFT frequency bins needs to be calculated. The symbol rate at the input of the FFT and the order of the FFT

will determine the frequency bin precision. Assume the input symbol rate is 2400 symbols per second and that the FFT order is 256, then the precision of the output frequency bins would be  $\frac{2400}{256} = 9.375$  Hz. The FFT output bins would cover a dynamic range of  $-1190.625$  Hz to  $1200$  Hz. A 256 point FFT would be very processor intensive to execute, and since the military standard only requires the single tone modem to cover a dynamic range of  $-75$  Hz to  $75$  Hz, only 19 of the 256 bins would be used. By using 19 bins, the doppler estimate would have a dynamic range of  $-84.375$  Hz to  $84.375$  with precision of  $9.375$  Hz. By taking a smaller FFT, the computation complexity would be drastically reduced, but the frequency bin precision drastically decreases. If a 16-point FFT is performed on the 2400 symbols per second signal, the resulting frequency bin precision would be  $\frac{2400}{16} = 150$  Hz. To compensate for this precision loss, a method of down-sampling can be performed prior to the FFT. Assume the new input symbol rate to the FFT is 300 symbols per second, then the frequency bin precision of the 16-point FFT becomes  $\frac{300}{16} = 18.75$  Hz and the dynamic range covered would be  $-131.25$  Hz to  $150$  Hz. By using 11 of the 16 bins, the doppler estimate would have a dynamic range of  $-93.75$  Hz to  $93.75$  with a precision of  $18.75$  Hz.

As discussed in section 2.1, the variable length preamble consists of 3 to 24 segments depending on the interleaver length. Assuming the initial correlation detects the first segment, 2 to 23 preamble segments will be received after the end of the current segment. These additional preamble segments can be used to avoid false acquisition. From the initial correlation and FFT, the timing position within the preamble segment is calculated. The terminal can use the timing position and the knowledge of the preamble to predict the number of correlations before the NSR will again dip below the threshold. If the next correlation which slides below the threshold matches the predicted, the preamble is declared as detected. After detection, the terminal transitions to the preamble tracking mode.

### 3.3.2 Preamble Tracking Mode

The preamble tracking mode determines the preamble count and autobaud information from the preamble. Once the preamble count is determined, this mode also keeps track of the

number of remaining preamble segments. As discussed in section 2.1, 2 of the 15 elements within a preamble segment contain the autobaud information and 3 of the 15 elements contain the preamble count. The preamble count indicates the number of preamble segments remaining before the end of the preamble.

The terminal uses the preamble timing position, determined during the preamble acquisition mode, to calculate the location of the two elements containing the autobaud information in the current preamble segment. To determine the autobaud information, a correlation between these elements and all possible options is completed. The option, from which the largest correlation peak is produced, is determined to be the correct data rate and interleaver length. Like the preamble acquisition mode, a method is used to minimize the possibility of error while detecting the autobaud information. These correlations are executed over each of the remaining preamble segments. The correlators increment a counter pertaining to the data rate and interleaver length detected in the current segment. At the end of the preamble, the option which produced the most maximum correlations is used to assign the data rate and interleaver length. This method allows for some receive errors and false positives to occur but is still able to choose the correct autobaud information.

Another correlation is performed at the three elements containing the preamble count information. Again, the option from which the largest correlation peak is produced is used as the preamble count value. Since the preamble can vary between 3 and 24 segments, the preamble count contains the number of preamble segments remaining to be received. To minimize the possibility of errors, this correlation is executed on consecutive preamble segments. If the preamble count on the next frame is one less than the preamble count on the current frame, the preamble count has most likely been determined without error.

Once the preamble count has been determined, the terminal continues to track the incoming preamble segments until the preamble count becomes zero. When the preamble count reaches zero, the terminal has detected the end of the preamble and transitions to the end of preamble mode.

### 3.3.3 End of Preamble Mode

During the end of preamble mode, the terminal uses the autobaud information to initialize the deinterleaver and decoder. Also calculated at this time is an initial channel estimate, using a least mean square (LMS) algorithm. The known end of the preamble is used along with the received signal to calculate the initial channel estimate. This channel estimate is used to initialize the coefficients for the matched filter, feedforward and feedback coefficients for the zero-forcing decision feedback equalizer (ZF-DFE).

To make calculations easier for the Single Tone receive data functionality, this mode also performs a timing adjustment. The initial timing position, calculated during initial acquisition, is used to determine the number of preamble and data samples present in the modem. The terminal makes an internal timing adjustment to ensure the preamble and data boundary occurs at a specific location to allow the data path to run more efficiently.

## 3.4 Data/Probe Functionality

Once the end of the preamble has been determined, rather than entering the Single Tone receive preamble functionality, the received signal takes the data/probe path after passing through the waveshaper. As shown in Figure 3.8, the block diagram of the data path includes a probe correlator, channel estimator, matched filter, an equalizer and demodulator, a descrambler, deinterleaver, decoder and an EOM detector. After passing through the EOM detector, the data bits are passed to the external interface.

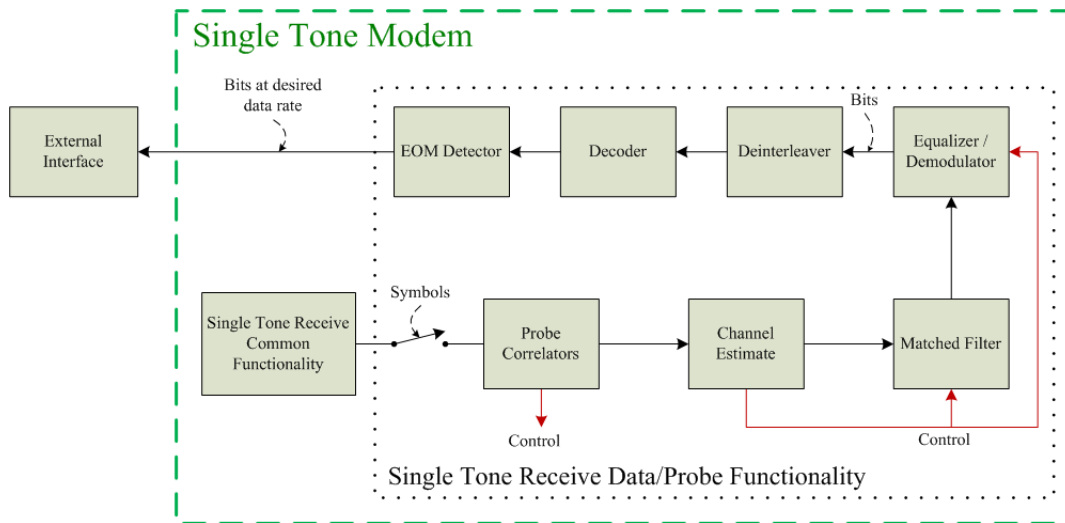


Figure 3.8 Single Tone Receive Data Functionality

### 3.4.1 Probe Correlators

The probe correlators use the timing position to calculate the magnitude of the correlation between the four signals from the waveshaper and the known transmitted probe sequence, as shown in Figure 3.9. From the correlation, the terminal chooses the ideal sample position, update the timing position, compute an SNR, check for signal dropout and monitor terminal clock differences.

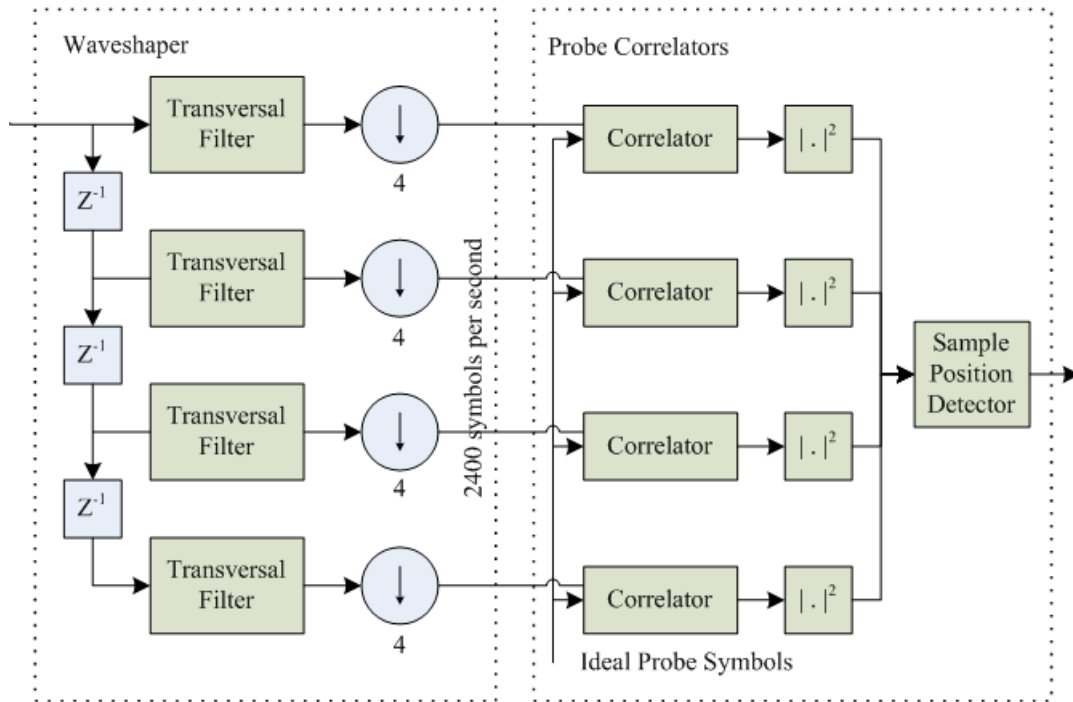


Figure 3.9 Probe Correlators

Since each of the four signals from the waveshaper is passed through the correlator, there are four correlation peaks, as shown in Figure 3.10. The sample position which produces the largest correlation peak is considered to be the best timing position. The remainder of the data path uses the signal associated with this sample position. In the example shown in Figure 3.10, the terminal would choose the signal with the third sample position since it produced the highest correlation peak.

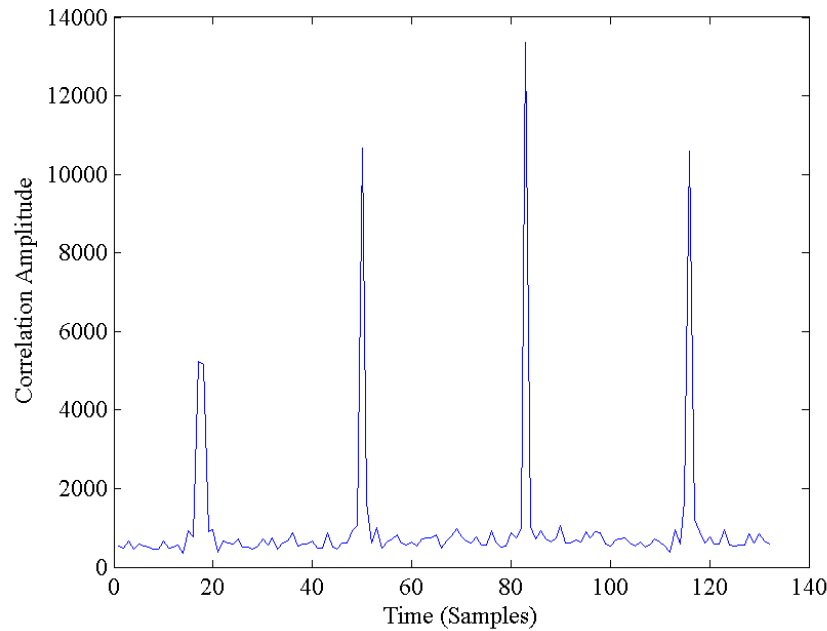


Figure 3.10 Probe Correlation with 4 Sample Positions

To update the timing position, the terminal calculates if the peak correlation occurred where it was expected. If it did not, the timing position can be updated from the new maximum peak location. The SNR can also be calculated and monitored. If the SNR drops below a threshold, the terminal declares that the signal is lost, regardless of whether or not an EOM has been detected.

When clock differences occur between the transmitting and receiving terminals, it can be observed during the probe correlations. As the clock drifts, the terminal sees the probe correlations change in magnitude. If the clocks were identical, the terminal would choose the ideal sample position during the initial data path execution and never have a need to change it. When the clocks differ, the terminal slowly sees the adjacent peaks change amplitude, eventually forcing the terminal to choose an adjacent peak as the new ideal sample position.



### 3.4.2 Channel Estimate

From Equation 3.2, the received signal is  $r_w[n] = \sum_{k=-\infty}^{\infty} I[k]h[n-k] + z[n]$ . The purpose of the receiving terminal is to estimate the transmitted symbol,  $I[n]$ . In order to estimate  $I[n]$ , an estimate of the channel effects,  $h[n]$ , needs to be calculated. One method that can be used to estimate  $h[n]$  is the LMS algorithm.

#### 3.4.2.1 LMS Algorithm

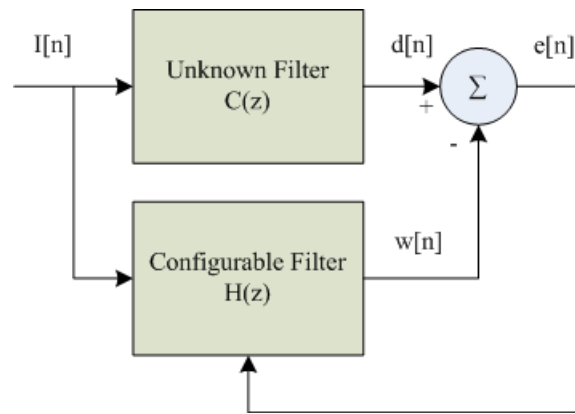


Figure 3.11 LMS Algorithm

A diagram to help describe the LMS algorithm is shown in Figure 3.11, where

- $I[n]$  is a known transmitted preamble or probe of length  $M$ ,
- $d[n]$  is the received preamble or probe of length  $M$ ,
- $c[n]$  are the unknown channel effects of length  $L + 1$ ,
- $h[n]$  are the configurable channel tap coefficients of length  $L + 1$ ,
- $w[n]$  is the filter output where  $w[n] = \sum_{k=0}^L I[k]h[n-k]$  of length  $M - L + 1$ ,
- $e[n]$  is the error between the received preamble or probe and the filter output where  $e[n] = d[n] - w[n]$  and is of length  $M - L + 1$

The LMS algorithm initializes the tap coefficients,  $\overline{h[n]}$ , to an initial value. The output of the filter and error are estimated and are used to update the new tap coefficients. Multiple iterations minimize the error,  $e[n]$ , and produce a known filter that closely resembles an unknown filter,  $C(z)$ . The steps to the LMS algorithm are shown below.

- Initialize filter coefficients,  $\mathbf{h}$ , to zero
- Calculate all  $M - L + 1$   $w[n]$ s where,  $w[n] = \sum_{k=0}^L I[k]h[n - k]$
- Calculate all  $M - L + 1$   $e[n]$ s where,  $e[n] = d[n] - w[n]$
- Calculate all  $L + 1$   $\mathbf{h}_{new}$ s where,

$$\begin{aligned}
 h_{new}[n] &= h[n] - \frac{1}{2}B \left[ \frac{d}{dh} \left[ E \left( |e[n]|^2 \right) \right] \right] \\
 &= h[n] - \frac{1}{2}B \left[ 2E \left( \frac{d}{dh} \left[ |e[n]|^2 \right] \right) \right] \\
 &= h[n] - B \left[ E \left( \frac{d}{dh} \left[ |e[n]|^2 \right] \right) \right] \\
 &= h[n] - B \left[ E \left( \frac{d}{dh} [e[n]e[n]^*] \right) \right] \\
 &= h[n] + B [I[n]e[n]^*]
 \end{aligned}$$

- Repeat all steps except the first initialization step

Once the  $L + 1$  taps of the channel estimate have been estimated,  $r_w[n]$  from Equation 3.2 can be rewritten as,

$$r_w[n] = \sum_{k=0}^L I[k]h[n - k] + z[n]$$

### 3.4.3 Matched Filter, Equalizer, and Demodulator

The first two blocks of the data path, the probe correlator and the channel estimator, produce control data by comparing the received signal with known probe data. The control data from the channel estimate is used to configure the matched filter, feedforward and feedback coefficients of the ZF-DFE.

### 3.4.3.1 Matched Filter

According to Proakis [5], the optimal demodulator can be realized as a matched filter to the channel estimate,  $h[n]$ , having impulse response  $h^*[-n]$  [5], as shown in Figure 3.12.

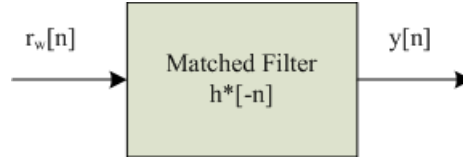


Figure 3.12 Matched Filter at the Receiver

Using Equation 3.1 where  $r_w[n] = I[n] \otimes h[n] + z[n]$ , the output of the matched filter,  $y[n]$ , can be defined as,

$$\begin{aligned}
 y[n] &= r_w[n] \otimes h^*[-n] \\
 &= (I[n] \otimes h[n] + z[n]) \otimes h^*[-n] \\
 &= I[n] \otimes h[n] \otimes h^*[-n] + z[n] \otimes h^*[-n]
 \end{aligned} \tag{3.3}$$

Let  $x[n] = h[n] \otimes h^*[-n]$ , where  $h[n]$  has non-zero values from  $0 \leq n \leq L$  and  $h^*[-n]$  has non-zero values from  $-L \leq n \leq 0$ . Then  $x[n]$  has non-zero values from  $-L \leq n \leq L$ , and

$$x[n] = \sum_{k=0}^L h^*[-k] h[n-k] \tag{3.4}$$

Then Equation 3.3 can be simplified to

$$\begin{aligned}
 y[n] &= I[n] \otimes x[n] + z[n] \otimes h^*[-n] \\
 &= \sum_{k=-L}^L I[k] x[n-k] + \sum_{k=-L}^0 z[k] h^*[-n-k] \\
 &= \sum_{k=-L}^{-1} I[k] x[n-k] + I[n] x[0] + \sum_{k=1}^L I[k] x[n-k] + \sum_{k=-L}^0 z[k] h^*[-n-k]
 \end{aligned} \tag{3.5}$$

The  $I[n]x[0]$  term is the desired symbol at the  $n$ th sample, the terms  $\sum_{k=-L}^{-1} I[k]x[n-k]$  and  $\sum_{k=1}^L I[k]x[n-k]$  represent ISI and  $\sum_{k=-L}^0 z[k]h^*[-n-k]$  is colored noise.

### 3.4.3.2 Zero-Forcing Decision Feedback Equalizer

The purpose of an equalizer is to reverse the channel effects. According to Proakis, the decision feedback equalizer (DFE) is comprised of two filters, a feedforward filter and a feedback filter, as shown in Figure 3.13. The purpose of the feedforward filter is to clean the symbols before entering the detector. The feedback filter removes ISI from the current detected symbol caused by previous symbol detection [5].

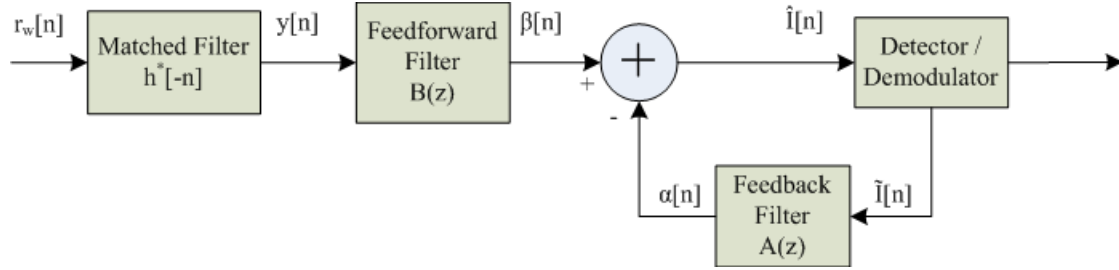


Figure 3.13 Matched Filter and Zero-Forcing Decision Feedback Equalizer

Where  $\hat{I}[n]$  is the estimate of the  $n$ th symbol and  $\tilde{I}[n]$  are previously detected symbols. The feedforward filter has  $K_1 + 1$  tap coefficients  $b[n]$  and the feedback filter has  $K_2$  tap coefficients  $a[n]$ . The output of the equalizer,  $\hat{I}[n]$ , can be defined as,

$$\hat{I}[n] = \beta[n] - \alpha[n] \quad (3.6)$$

Using Equation 3.5,  $y[n] = I[n] \otimes x[n] + z[n] \otimes h^*[-n]$ , where  $y[n]$  is the output of the matched filter. Then, the output of the feedforward filter,  $\beta[n]$ , can be defined as,

$$\begin{aligned} \beta[n] &= y[n] \otimes b[n] \\ &= (I[n] \otimes x[n] + z[n] \otimes h^*[-n]) \otimes b[n] \\ &= I[n] \otimes x[n] \otimes b[n] + z[n] \otimes h^*[-n] \otimes b[n] \end{aligned} \quad (3.7)$$

Let  $q[n] = x[n] \otimes b[n]$ , where  $x[n]$  has non-zero values from  $-L \leq n \leq L$  and  $b[n]$  has non-zero values from  $-K_1 \leq n \leq 0$ . Then  $q[n]$  has non-zero values from  $-K_1 - L \leq n \leq L$  and

$$q[n] = \sum_{k=-K_1}^0 x[k]b[n-k] \quad (3.8)$$

Then the output of the feedforward filter, can be simplified using the definition of  $q[n]$  and Equation 3.7.

$$\begin{aligned} \beta[n] &= I[n] \otimes q[n] + z[n] \otimes h^*[-n] \otimes b[n] \\ &= \sum_{k=-L-K_1}^L I[k]q[n-k] + z[n] \otimes h^*[-n] \otimes b[n] \\ &= \sum_{k=-L-K_1}^{-1} I[k]q[n-k] + I[n]q[0] + \sum_{k=1}^L I[k]q[n-k] + z[n] \otimes h^*[-n] \otimes b[n] \quad (3.9) \end{aligned}$$

The  $I[n]q[0]$  term is the desired symbol at the  $n$ th sample, the terms  $\sum_{k=-L-K_1}^{-1} I[k]q[n-k]$  and  $\sum_{k=1}^L I[k]q[n-k]$  represent ISI and  $z[n] \otimes h^*[-n] \otimes b[n]$  is colored noise. Now Equation 3.6, or the output of the equalizer, can be expanded using Equation 3.9.

$$\hat{I}[n] = I[n]q[0] + \sum_{k=-L-K_1}^{-1} I[k]q[n-k] + \sum_{k=1}^L I[k]q[n-k] + z[n] \otimes h^*[-n] \otimes b[n] - \alpha[n] \quad (3.10)$$

The output of the feedback filter,  $\alpha[n]$ , can be defined as,

$$\begin{aligned} \alpha[n] &= \tilde{I}[n] \otimes a[n] \\ &= \sum_{k=1}^{K_2} \tilde{I}[k]a[n-k] \quad (3.11) \end{aligned}$$

Then the output of the equalizer can be expanded further using the output of the feedback filter, Equation 3.11, and Equation 3.10.

$$\begin{aligned} \hat{I}[n] &= I[n]q[0] + \sum_{k=-L-K_1}^{-1} I[k]q[n-k] + \sum_{k=1}^L I[k]q[n-k] + z[n] \otimes h^*[-n] \otimes b[n] \\ &\quad - \sum_{k=1}^{K_2} \tilde{I}[k]a[n-k] \quad (3.12) \end{aligned}$$

The purpose of a zero-forcing equalizer is to minimize the effects of ISI. To do this, the feedforward and feedback coefficients need to be initialized using certain conditions. Assume  $K_2 \leq L$  then Equation 3.12 can be expanded as,

$$\begin{aligned}
\hat{I}[n] &= \sum_{k=-L-K_1}^{-1} I[k]q[n-k] + I[n]q[0] + \sum_{k=1}^{K_2} I[k]q[n-k] + \sum_{k=K_2+1}^L I[k]q[n-k] \\
&\quad + z[n] \otimes h^*[-n] \otimes b[n] - \sum_{k=1}^{K_2} \tilde{I}[k]a[n-k] + \left[ \sum_{k=1}^{K_2} \tilde{I}[k]q[n-k] - \sum_{k=1}^{K_2} \tilde{I}[k]q[n-k] \right] \\
&= \sum_{k=-L-K_1}^{-1} I[k]q[n-k] + I[n]q[0] + \sum_{k=K_2+1}^L I[k]q[n-k] + z[n] \otimes h^*[-n] \otimes b[n] \\
&\quad + \sum_{k=1}^{K_2} (I[k] - \tilde{I}[k])q[n-k] - \sum_{k=1}^{K_2} \tilde{I}[k](q[n-k] - a[n-k]) \tag{3.13}
\end{aligned}$$

Assume that the detector is making good decisions, such that  $\tilde{I}[n] = I[n]$ , and assign the  $K_2$  feedback coefficients,  $a[n]$ , to

$$a[n] = q[n] \tag{3.14}$$

where  $q[n]$  is defined in Equation 3.8, then Equation 3.13 can be reduced to,

$$\hat{I}[n] = \sum_{k=-L-K_1}^{-1} I[k]q[n-k] + I[n]q[0] + \sum_{k=K_2+1}^L I[k]q[n-k] + z[n] \otimes h^*[-n] \otimes b[n]$$

The ISI is reduced to  $\sum_{k=-L-K_1}^{-1} I[k]q[n-k]$  and  $\sum_{k=K_2+1}^L I[k]q[n-k]$ . To completely eliminate the ISI, the feedforward coefficients need to be assigned such that,

$$q[n] = \begin{cases} 1 & \text{for } n = 0 \\ 0 & \text{for } -L - K_1 \leq n \leq -1 \text{ and } K_2 + 1 \leq n \leq L \end{cases}$$

Assume that  $K_1 \geq L$  and define the following vectors and matrices,

$$\mathbf{q} = \begin{bmatrix} q[-K_1 - L] \\ q[-K_1 - L + 1] \\ \vdots \\ q[-K_1] \\ q[-K_1 + 1] \\ \vdots \\ q[-L - 1] \\ q[-L] \\ \vdots \\ q[L - K_1] \\ q[L - K_1 + 1] \\ \vdots \\ q[-1] \\ q[0] \\ q[K_2] \\ q[K_2 + 1] \\ \vdots \\ q[L] \end{bmatrix} = \begin{bmatrix} 0 \\ 0 \\ \vdots \\ 0 \\ 0 \\ \vdots \\ 0 \\ 0 \\ \vdots \\ 0 \\ 0 \\ \vdots \\ 0 \\ 1 \\ 0 \\ 0 \\ \vdots \\ 0 \end{bmatrix}, \mathbf{b} = \begin{bmatrix} b[-K_1] \\ b[-K_1 + 1] \\ \vdots \\ b[-1] \\ b[0] \end{bmatrix}$$

$$\mathbf{X} = \begin{bmatrix} x[-L] & x[-L-1] & \cdots & x[-L-K_1+1] & x[-L-K_1] \\ x[-L+1] & x[-L] & \cdots & x[-L-K_1+2] & x[-L-K_1+1] \\ \vdots & \vdots & \ddots & \vdots & \vdots \\ x[0] & x[-1] & \cdots & x[-K_1+1] & x[-K_1] \\ x[1] & x[0] & \cdots & x[-K_1+2] & x[-K_1+1] \\ \vdots & \vdots & \ddots & \vdots & \vdots \\ x[K_1-L-1] & x[K_1-L-2] & \cdots & x[-L] & x[-L-1] \\ x[K_1-L] & x[K_1-L-1] & \cdots & x[-L+1] & x[-L] \\ \vdots & \vdots & \ddots & \vdots & \vdots \\ x[L] & x[L-1] & \cdots & x[L+1-K_1] & x[L-K_1] \\ x[L+1] & x[L] & \cdots & x[L+2-K_1] & x[L+1-K_1] \\ \vdots & \vdots & \ddots & \vdots & \vdots \\ x[K_1-1] & x[K_1-2] & \cdots & x[0] & x[-1] \\ x[K_1] & x[K_1-1] & \cdots & x[1] & x[0] \\ x[K_2+K_1] & x[K_2+K_1-1] & \cdots & x[K_2+1] & x[K_2] \\ x[K_2+K_1+1] & x[K_2+K_1] & \cdots & x[K_2+2] & x[K_2+1] \\ \vdots & \vdots & \ddots & \vdots & \vdots \\ x[K_1+L] & x[K_1+L-1] & \cdots & x[L+1] & x[L] \end{bmatrix}$$

Where  $\mathbf{q}$  is a  $2L + K_1 - K_2$  vector of the desired response,  $\mathbf{b}$  is a  $K_1 + 1$  vector of the configurable feedforward coefficients, and  $\mathbf{X}$  is a  $2L + K_1 - K_2$  by  $K_1 + 1$  matrix of the channel estimate's autocorrelation, then  $\mathbf{q} = \mathbf{X}\mathbf{b}$ . There are  $2L + K_1 - K_2$  equations with  $K_1 + 1$  unknowns. To simplify,  $K_1 + 1$  of the  $2L + K_1 - K_2$  equations can be chosen. Note that  $x[n]$  has non-zero values over the range  $-L \leq n \leq L$ , so it seems most logical to choose  $q[-K_1]$  through  $q[0]$ . Then  $\mathbf{q}$  and  $\mathbf{X}$  can be simplified to create a subset of  $K_1 + 1$  equations to solve.



$$\mathbf{q}_{simplified} = \begin{bmatrix} q[-K_1] \\ q[-K_1 + 1] \\ \vdots \\ q[-L - 1] \\ q[-L] \\ \vdots \\ q[L - K_1] \\ q[L - K_1 + 1] \\ \vdots \\ q[-1] \\ q[0] \end{bmatrix} = \begin{bmatrix} 0 \\ 0 \\ \vdots \\ 0 \\ 0 \\ \vdots \\ 0 \\ 0 \\ \vdots \\ 0 \\ 1 \end{bmatrix}$$

$$\mathbf{X}_{simplified} = \begin{bmatrix} x[0] & x[-1] & \cdots & x[-K_1 + 1] & x[-K_1] \\ x[1] & x[0] & \cdots & x[-K_1 + 2] & x[-K_1 + 1] \\ \vdots & \vdots & \ddots & \vdots & \vdots \\ x[K_1 - L - 1] & x[K_1 - L - 2] & \cdots & x[-L] & x[-L - 1] \\ x[K_1 - L] & x[K_1 - L - 1] & \cdots & x[-L + 1] & x[-L] \\ \vdots & \vdots & \ddots & \vdots & \vdots \\ x[L] & x[L - 1] & \cdots & x[L + 1 - K_1] & x[L - K_1] \\ x[L + 1] & x[L] & \cdots & x[L + 2 - K_1] & x[L + 1 - K_1] \\ \vdots & \vdots & \ddots & \vdots & \vdots \\ x[K_1 - 1] & x[K_1 - 2] & \cdots & x[0] & x[-1] \\ x[K_1] & x[K_1 - 1] & \cdots & x[1] & x[0] \end{bmatrix}$$

The feedforward coefficients,  $b[n]$ , need to be assigned such that,

$$\begin{aligned} \mathbf{q}_{simplified} &= \mathbf{X}_{simplified} \mathbf{b} \\ \mathbf{b} &= \mathbf{X}_{simplified}^T \mathbf{q}_{simplified} \end{aligned} \quad (3.15)$$

To minimize processing, the LMS algorithm could be used to initialize the feedforward coefficients where  $\mathbf{b}$  would be the configurable tap coefficients,  $\mathbf{X}$  would be the ideal input, and  $\mathbf{q}$  would be the desired response. The implementation discussed above documents the current implementation, but can be improved.

### 3.4.3.3 Detector / Demodulator

The detector receives the equalized symbol,  $\hat{I}[n]$ , and compares it with the ideal constellation diagram. The ideal symbol which minimizes the Euclidean distance to the equalized symbol is selected as the detected symbol,  $\tilde{I}[n]$ . This detected symbol is then used in the feedback loop of the ZF-DFE, as  $\tilde{I}[n]$ .

Opposite of the modulator, the demodulator translates the detected symbols into soft decisions. If the decoder incorrectly chooses the detected symbol, the gray decoding minimizes bit errors by having neighboring symbols on the constellation diagram differ by one bit. The soft decisions are then passed to the deinterleaver.

### 3.4.4 Deinterleaver, Decoder, and EOM Detector

The deinterleaver performs the opposite operation of the interleaver. It descrambles the received data bits, scattering burst errors across multiple code words to make it possible for the decoder to correct the errors. Similar to the interleaver, the incoming data bits are placed into columns in a specific order. Once the deinterleaver is full, the bits are unloaded by rows. After deinterleaving, the bits are passed to the decoder.

A viterbi decoder is used to decode the FEC encoded data bits. The decoded data bits from the viterbi decoder are passed to the EOM detector. The EOM detector performs a correlation between the bits from the decoder and the known EOM sequence. If the resulting correlation peak is larger than or equal to the EOM detection threshold, the EOM has been detected. Typically the EOM threshold is set such that no bit errors are allowed in the received EOM. If the EOM is not successfully detected, the terminal eventually detects a signal loss when the probe correlators see the SNR drop below a threshold.

## CHAPTER 4. ISOLATION OF THE SOFTWARE DEFECT USING BIT ERROR TIMING AND CHANNEL EFFECTS

After the channel model and receive path are understood, the next step in debugging the Single Tone modem is isolating the software defect. By using the timing of bit errors, and applying channel effects individually, the debugging efforts can be focused to a certain area of software. The timing of bit errors can reveal a lot about the location of the problem. Bit errors which occur at the beginning of the reception indicate a different software defect, than bit errors occurring at the end. If bit errors occur during the middle of the reception, typically more information needs to be obtained to further determine the area of software to debug. To obtain more information, channel effects are applied individually to allow the software defects associated with each channel effect to be isolated and debugged.

### 4.1 Software Isolation using Bit Error Timing

Bit errors which occur during testing, may have a repeatable timing pattern that may help to isolate the software issue. Each bit error position leads to a different section of code to help begin the debugging process.

#### 4.1.1 Errors at the Beginning of the Reception

If bit errors occur at the beginning of the reception, the area of code to begin debugging is the preamble path. As discussed in Section 3.3, there are three modes of the preamble path including acquisition, tracking and end of preamble detection. Bit errors at the beginning of the reception indicate that the preamble path is the source of the defect, but does not give enough information to positively determine in which preamble path mode the issue occurs.

### Preamble Path - Preamble Acquisition Mode: Preamble Correlators

As discussed in Section 3.3.1, the main purpose of the preamble acquisition mode is to detect the preamble, and calculate initial timing position and doppler shift. The terminal typically has a method in place within the preamble correlators to avoid false detection. The method previously discussed uses the maximum correlation from two consecutive preamble segments and the timing between them to avoid false detection. This method helps to avoid false detection, but cannot completely prevent it. If the bit errors at the beginning of the reception are seen on a regular basis, false detection is not the issue, since it would not occur regularly. If the errors observed occur occasionally, false detection could be the issue and the incoming data should be captured. Use the captured data to step through the software and observe the correlation peaks throughout the received signal. Although the probability is low, the received signal could have random data that is similar enough to the preamble that it produces two correlator peaks with a low enough NSR to pass the threshold. By forcing the code to ignore the original correlator peaks, it may be seen that a correlator peak with much lower NSR occurs further into the reception.

The second purpose of the preamble acquisition mode is to calculate an initial timing position from the output of the preamble correlation. The initial timing position is calculated by comparing the index of the maximum correlation peak to the known preamble. It would be easy to miscalculate and misuse the timing position. Assume a piece of the preamble sequence looks like Equation 4.1, where each entry within  $I[n]$  represents a preamble element.

$$I[n] = [7\ 2\ 1\ 4\ 0\ 0\ 0\ 0\ 0\ 0\ 0\ 0\ 3\ 5\ 6] \quad (4.1)$$

Assume the received signal is given in Equation 4.2,

$$d[n] = [0\ 0\ 0\ 3\ 5\ 6\ 7\ 2\ 1\ 4\ 0\ 0\ 0\ 0] \quad (4.2)$$

Table 4.1 shows an example of a correlation between the received signal and the sequence 7 2 1 4.

Table 4.1 Preamble Sequence Example

d	[0]	[1]	[2]	[3]	[4]	[5]	[6]	[7]	[8]	[9]	[10]	[11]	[12]	[13]	[14]	[15]
Value	0	0	0	3	5	6	7	2	1	4	0	0	0	0	0	0
n=0	7	2	1	4												
n=6							7	2	1	4						
n=12													7	2	1	4

From Table 4.1, the maximum correlation occurs at  $n = 6$ . If the receiving terminal was expecting the 7 2 1 4 sequence to occur at indices [0], [1], [2], and [3], respectively, then the initial timing indicates the received signal is six indices off from the expected. One needs to make sure that the method used to indicate the initial timing is throughout the entire receive path.

#### **Preamble Path - Preamble Acquisition Mode: FFT**

The preamble acquisition mode also calculates the initial doppler shift. To calculate the initial doppler shift, an FFT is performed on the correlation between the received signal and known preamble. The precision of each frequency bin depends on the incoming sample rate, and the order of FFT. This doppler shift estimate is fed into the translator and the preamble is re-correlated. If an incorrect doppler shift estimate is calculated, the re-correlation produces smaller peaks than the original correlation.

#### **Preamble Path - Preamble Tracking Mode: Preamble Count Correlators**

As discussed in Section 3.3.2, the preamble tracking mode determines the preamble count and uses it to determine when the last preamble segment is received. The terminal typically has a method in place within the preamble count correlators to avoid false calculation. The method previously discussed uses the preamble count captured in two consecutive preamble segments and performs a check to see if the later count is one less than the earlier. This method helps avoid false detection, but cannot completely prevent it. If the bit errors at the beginning of the reception are seen on a regular basis, false preamble count detection is not the issue, since false detection would not occur regularly. If the errors occur occasionally, false

preamble count detection could be the issue and the incoming data should be captured. The preamble count for each segment can be calculated if the interleaver length of the transmitting terminal is known. A short interleaver produces 3 preamble segments and a long interleaver produces 24 segments. By stepping through the code a comparison can be made between the preamble count determined from the received signal and the known preamble count. Although the probability is low, the received signal could have bit errors occur such that the preamble count from two consecutive segments have a difference of one, but are still incorrect.

### **Preamble Path - End of Preamble Mode: Initialization for Data Mode**

Section 3.3.3 describes the end of preamble mode. A major function of the end of preamble mode is calculating a channel estimate and adjusting the timing position of the received signal. During the end of preamble mode, an initial channel estimate is performed, to be used on the first data frame. The channel estimate is calculated using the LMS algorithm discussed in Section 3.4.2.1. The first step to ensure that the channel estimate is being calculated correctly is to check the software logic against the LMS algorithm. Using Equation 4.1 and Section 3.4.2.1 as a reference,  $w[n] = \sum_{k=0}^L I[k]h[n-k]$  and,

$$w[I[3]] = h[0]I[3] + h[1]I[2] + h[2]I[1] + h[3]I[0]$$

Following the LMS algorithm outlined, Equation 4.2 can be used to calculate  $e[n]$ , where  $d[I[3]]$  is located at index  $d[9]$ .

$$\begin{aligned} e[I[3]] &= d[I[3]] - w[I[3]] \\ &= d[9] - w[I[3]] \end{aligned}$$

It would be very easy to use the wrong indices when calculating the channel estimate. For instance, rather than using the received symbol thought to be  $I[3]$ , perhaps  $d[I[2]]$  is used instead. The software implementing this algorithm needs to be checked very thoroughly. The initial channel estimate is only used for the first frame of data, so bit errors occurring at the beginning may be caused by an error in the LMS logic.

### 4.1.2 Errors at the End of the Reception

If bit errors occur at the end of the reception, the area of code to begin debugging is the data path. As discussed in Section 3.4, the receive path contains a probe correlator, channel estimator, matched filter, an equalizer and demodulator, a descrambler, deinterleaver, decoder and an EOM detector. The main focus for errors occurring at the end of a reception is the EOM detector. As discussed in Section 3.4.4, only the data bits prior to the EOM are sent to the external interface.

#### Data Path - EOM Detector

One possible cause of bit errors may be related to bit boundary differences between the transmitting and receiving terminals. For example, if the implementation of the transmitting terminal is limited to 16-bit boundaries, rather than 8-bit boundaries, the valid data bits must be zero-padded before the EOM is attached. If this is occurring the receiving terminal will see less than 16 bits of padding prior to the EOM. Since the logic assumes all bits prior to the EOM are valid, the extra zeros are sent to the external interface and logged as errors. The only method to check if this is occurring is to check the decoder output. By sending all ones, the data directly before the EOM should be ones, rather than zero-padding. If the data is zero-padded, there is nothing the engineer can do except make a design change.

Another potential issue which causes bit errors at the end of the reception is the EOM detection logic. The terminal may rely on the probe correlators to detect a signal loss and mark the end of the reception, if the logic for EOM detection is incorrect. Bit errors could occur if the EOM or data past the EOM is sent to the external interface. By checking the output of the decoder, it can be determined whether or not the EOM is present. If the EOM is never seen within the decoded bits, there may be a mismatch between the number of interleaver flush bits sent by the transmitting terminal and the number of flush needed by the receiving terminal.

### 4.1.3 Errors Throughout the Reception

If bit errors occur throughout the reception, both the preamble and data paths have potential areas of interest. They include the initial doppler shift estimate within the preamble acquisition mode, autobaud detection within the preamble tracking mode, the timing adjustment performed during the end of preamble mode, and the deinterleaver with the data path.

#### **Preamble Path - Preamble Acquisition Mode: FFT**

According to the MIL-STD-188-110A [3], the single tone modem is only required to compensate for a doppler shift of 75 Hz. Within the preamble acquisition mode, an initial doppler shift estimate is performed by placing the correlation of the received signal and the known preamble through an FFT. If the doppler shift is determined to be larger than 75 Hz, the terminal will only correct for 75 leading to bit errors and loss of synchronization. By checking the output of the FFT, it can be determined if the doppler shift is greater than 75 Hz. If it is, corrections need to be made within the test equipment to stay within the military specifications.

#### **Preamble Path - Preamble Tracking Mode: Autobaud Information Correlators**

During preamble tracking mode, the terminal correlates on all possible interleaver length and data rate options to see which produces the greatest correlation peak. If the logic to determine the autobaud information is wrong, the incorrect data rate or interleaver length would cause bit errors throughout the reception. Compare the detected autobaud information with the known transmitting terminal's data rate and interleaver length to determine if they were correctly received.

#### **Preamble Path - End of Preamble Mode: Timing Adjustment**

The other task performed by the end of preamble mode is a timing adjustment. From Table 4.1, it was shown that the received signal was offset by six. To make data mode easier, the received signal is internally shifted such that the boundary between the end of preamble and data has an offset of zero. When performing this function, it is easy to make a mistake associated with array indices. It is also easy to request an incorrect amount of samples from the receiver during the first frame of data, since a portion of the first data frame was received



during the final preamble segment. Stepping through the software to check all logic is correct is a quick and easy method to ensure a correct timing adjustment.

### **Data Path - Deinterleaver**

If the bit errors are caused by the deinterleaver on the data path, it would be easy to identify. The bit errors seen during the reception typically occur in a periodic manner and the period may resemble the length of the selected deinterleaver. If the period does resemble the deinterleaver length, one area of interest may be the logic within the deinterleaver which switches between loading and unloading.

When bit errors occur during the beginning or the end of a reception, there are fewer possible software issues, than when they occur in the middle of the reception. Typically, more information needs to be obtained to further determine the area of software to debug. The bit errors may be related to an AGC frequency dispersion issue. Perhaps the probe correlators are not choosing the correct peak for time dispersion. There are many more blocks within the data path that may be contributing to the bit errors received in the middle of the reception, but more debug information is needed. Another method of capturing debug information is to isolate the individual channel effects. By isolating each channel effect, software defects associated with each issue are easier to isolate and debug.

## **4.2 Software Isolation using Channel Effects**

In addition to using bit error timing to isolate the software issue, applying channel effects individually is another method that should be used. Bit errors which occur because of terminal clock differences indicate a different software issue than bit errors caused by frequency dispersion. By isolating individual channel effects, software defects relating to each can be debugged before combining them together for performance testing.

It is generally easier to isolate the individual channel effects if the transmit and receive software can be placed in an 8k sps loopback mode. By placing the modem in 8k sps loopback, the Single Tone modem software is completely isolated, yet the entire modem is tested. To accomplish this, a loop is placed at the output of the transmit rate change filter to the

input of the receive rate change filter. This can eliminate some of the effects of using multiple radios, such as terminal clock differences and doppler shift. The loopback also allows the engineer to simulate doppler shift, terminal clock differences, noise, frequency and time dispersion independently.

#### 4.2.1 Doppler Isolation

Doppler shift is caused by the relative movement of either the transmitting or receiving terminal. It causes a frequency change to occur on the signal that the receiving terminal is not expecting.

##### Simulation

As discussed in Section 2.2, the transmit translator shifts the complex signal by +1800 Hz and converts it into a real signal. The output of the translator results in a 3 kHz bandwidth signal, centered at 1800 Hz and can be seen in Figure 2.6. To simulate a doppler shift, test code can be added to the transmit translator to shift the signal 1800 Hz plus a doppler shift. The top image in Figure 4.1 shows the output of the transmit translator with a doppler shift of 0 Hz. The bottom image shows an offset of 70 Hz.

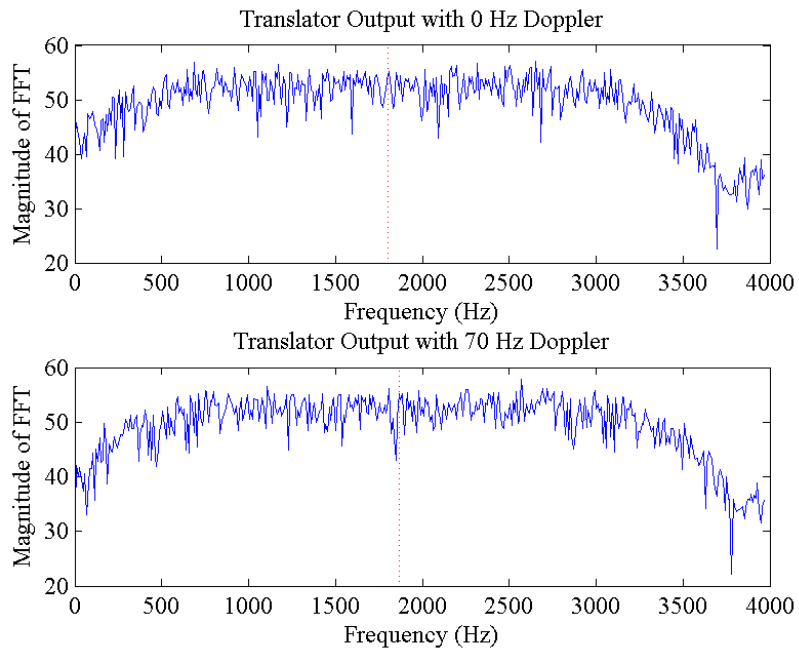


Figure 4.1 Frequency Domain of the Translator Output with 0 and 70 Hz Doppler

### Receive Software Expectations

On the receive path, the doppler shift estimate is calculated from the FFT output of the correlation between the received signal and the known preamble sequence. If the doppler shift is 70 Hz, the maximum peak correlation should occur in the bin representing 75 Hz. Figure 4.2 shows the output of the FFT with a doppler shift of 0 Hz and 70 Hz.

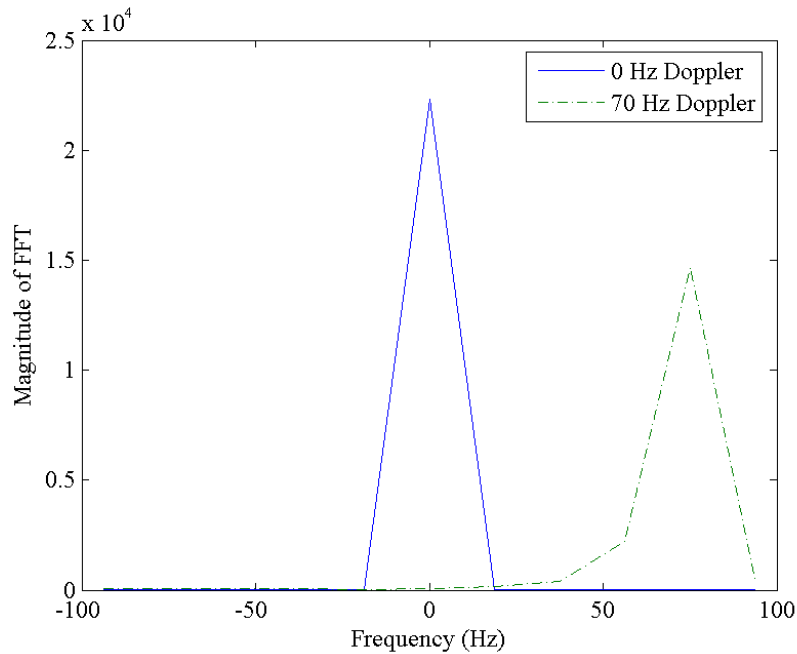


Figure 4.2 Acquisition FFT Output with 0 and 70 Hz Doppler

By using the 8k sps audio loopback, the doppler shift can be set and controlled on the transmit translator. All doppler shift ranges can be tested from  $-75$  Hz to  $75$  Hz and the calculated offset on the receive FFT can be compared to the known value set at the modified transmit translator. Loopback mode can hide some interoperability errors with existing radios and should be used as one method of debugging. After all errors seen in loopback mode are corrected, the engineer should retest the software by using an existing radio such as a Q-9604 or an MDM-3001.

If the FFT output does not resemble the expected doppler shift estimate, and the doppler shift is large enough to be seen in the frequency domain at the output of the transmit translator, check both the output of the transmit translator and the input to the receive translator. If the two graphs do not match, there is probably an error in the rate change filter. If the two graphs are the same and the doppler shift can be seen in both, the section of software to begin debugging is the receive translator, waveshaper, down-sampling prior to the FFT, and the FFT implementation.

### 4.2.2 Terminal Clock Difference Isolation

Terminal clock differences occur whenever the transmitting and receiving terminals are not using the same clock. One clock is faster or slower in reference to the other clock, causing drift in the signal which the receiving terminal is not expecting.

#### Simulation

A method of inducing clock drift in 8k sps loopback mode is to add test code to the transmit rate change filter. The transmit rate change filter converts the 9.6k sps audio signal to an 8k sps audio signal by first up-sampling by 10 to create a signal at 96k sps. Then the signal is down-sampled by 12 to create a signal at 8k sps. To create the illusion of clock drift, create test code to either add or subtract a sample every second from the 96k sps signal.

#### Receive Software Expectations

Clock drift can easily be detected at the receive probe correlators. As described in Section 3.4.1, the probe correlators determine the ideal sample position by correlating each of the four sample positions with the known probe sequence. At the output of the probe correlator, there are four correlation peaks as shown in Figure 3.10. One has a maximum amplitude, the two adjacent peaks have roughly equal magnitude and the final peak has the smallest magnitude. If the signal is drifting due to terminal clock differences, the probe correlations will change over time. One of the two adjacent peaks will gain amplitude, while the other will lose. Eventually, the original adjacent peak will take over as the maximum correlation peak, while the initial maximum peak will become an adjacent peak. Figure 4.3 shows this transition.

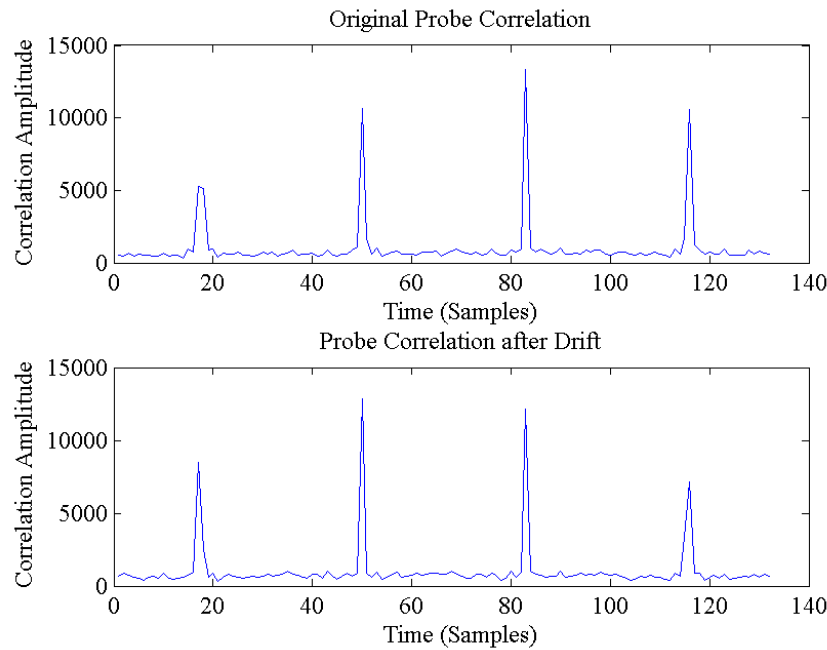


Figure 4.3 Original Probe Correlation and after Drift

As shown in Figure 4.3, the original probe correlation can be seen at the top image. The maximum correlation peak occurs at the third sample position, while the second and fourth peaks contain roughly equal power. As clock drift occurs, the second peak grows in power, while the other adjacent peak weakens in power. The bottom image in Figure 4.3 shows the second peaks growing enough in power to pass the third peak to become the new ideal sample position.

One common method to solve clock drift is to force the probe correlations to stay stationary. By monitoring the probe correlation peaks, samples can be added or subtracted in the receive rate change filter. Correlation peak fluctuate naturally. Be sure a method is in place to ensure any peak changes are not just natural fluctuations. For instance, when one of the two adjacent peaks is a certain percentage higher than the other for a pre-determined time, the software knows it is not natural fluctuation and signals the rate change filter that drift is occurring. If the leading adjacent peak is greater than the lagging, then the receiving terminal's clock is running slower than the transmitting terminal's clock. To compensate for this difference the

receive rate change filter drops samples to advance ahead and speed up the receive clock. If the lagging adjacent peak is growing larger than the leading, then the receiving terminal's clock is running faster than the transmitting terminal's clock. The receive rate change filter adds samples to slow the receive clock as a method to compensate.

If the receiving terminal detects a signal loss, or the engineer observes the correlation peaks changing in the debugger, this indicates that the logic to correct for terminal clock differences is not working. First, check that the receive rate change filter is being instructed the same command as the transmit rate change filter. If the test code is simulating clock drift by slowing down the transmit clock, then the logic which keeps track of the adjacent correlator peaks should instruct the receive rate change filter to also slow down. If the opposite command is being given to the receive rate change filter, the engineer should begin debugging the logic maintaining the adjacent correlator peaks.

The frequency of altering the transmit and receive clocks within the rate change filters should also be checked. If the test code within the transmit rate change filter is adding or subtracting one sample per second, then the receive rate change filter should also be adding or subtracting at roughly the same rate. If the frequencies are not similar, the logic within the probe correlators which determines how frequently the receive rate change filter is called needs to be modified.

### 4.2.3 Noise Isolation

Noise occurs over any channel and can be thought of as a source of an additive random signal. In the case of Single Tone, it is assumed to be AWGN.

#### Simulation

Two methods of simulating noise, frequency dispersion and time dispersion are: using a software channel simulator in 8k sps loopback mode, and using an existing modem as a channel simulator in audio mode. The first method inserts a software channel simulator within the 8k sps audio loopback mode. The second method takes the modem software out of 8k sps loopback mode, and uses two external, existing modems. Two examples of existing modems that could

be used are a Q-9604 and an MDM-3001. As an example hardware configuration, a Q-9604 can be used as a transmitting terminal, while the MDM-3001 can be placed between the Q-9604 and the modem software under test and configured to an HF channel simulator mode. Since the modem software under test needs to be taken out of the 8k sps loopback mode and uses two other external terminals, this method should only be used if the engineer is confident that all doppler shift and terminal clock issues have already been resolved.

### **Receive Software Expectations**

On the receive data path, the major components for controlling bit errors seen on data are the matched filter, equalizer/demodulator, deinterleaver, and decoder. Unfortunately, the equalizer used in the Single Tone modem is a ZF-DFE which enhances noise, so the equalizer/demodulator does not help a signal recover from AWGN.

The effects of AWGN can be seen in the receive constellation diagrams. Figure 2.4 shows the original constellation diagram of the transmitted signal. Figure 4.4 shows the constellation diagram at the output of the equalizer for a channel SNR of 40 and 15 dB. In noisier channels, the constellation diagram becomes fuzzier.



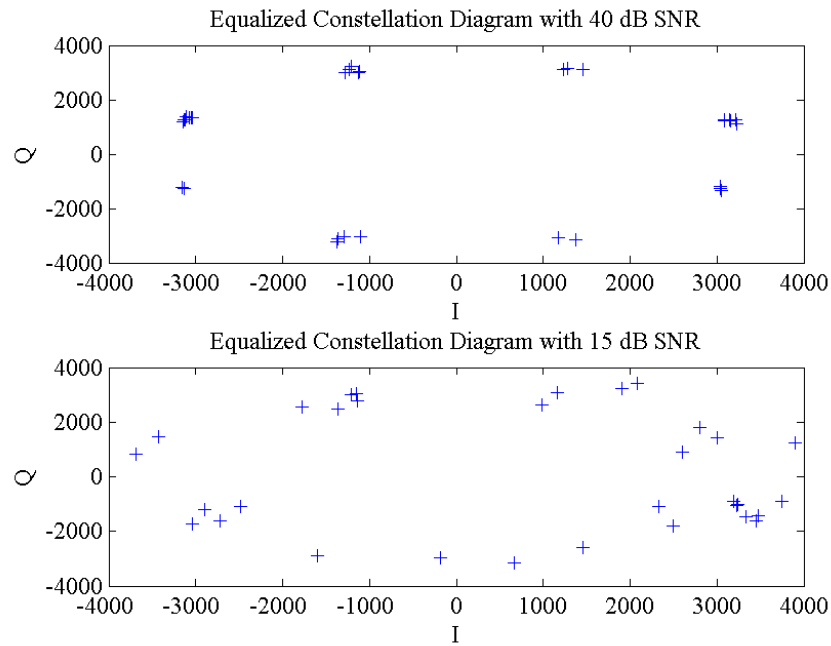


Figure 4.4 Equalized Constellation Diagram with 40 dB and 15 dB SNR

Euclidean distance is used within the demodulator to map the received symbols to bits, or soft decisions. In noisier channels, the Euclidean distance is significantly greater between the received and the ideal symbols. If the Euclidean distance is large enough, the demodulator may choose a neighboring symbol, rather than the ideal symbol. Since gray encoding is used, if a neighboring symbol is chosen instead of the ideal, only one bit error will occur in that group of bits.

As described, in Section 2.2, interleavers have no advantage in channels which contains only AWGN, since bit errors occur randomly throughout the channel. The only component to correct bit errors caused by noise is the viterbi decoder. If bit errors are seen in channels where only AWGN is present, the logic in the viterbi decoder is the software of interest for debugging.

#### 4.2.4 Frequency Dispersion Isolation

The ionosphere absorbs signal energy at different rates, depending on the density of the ionosphere. Since the rate at which energy is absorbed is not constant, it causes varying signal amplitudes, or frequency dispersion.

##### **Simulation**

As discussed in Section 4.2.3, there are two methods to simulate frequency dispersion. Assuming the doppler shift and terminal clock difference issues have already been resolved, the second method using two existing radios is preferred. Frequency dispersion is a time-varying fade which causes the average input signal level to the terminal to vary. Unfortunately, within channel simulators, only the frequency of the fade, not the magnitude, is configurable.

##### **Receive Software Expectations**

Frequency dispersion can be seen on the amplitude on the incoming signal. Figure 4.5 shows the average magnitude of the input signal to the terminal with 0 and 5 Hz of frequency dispersion.

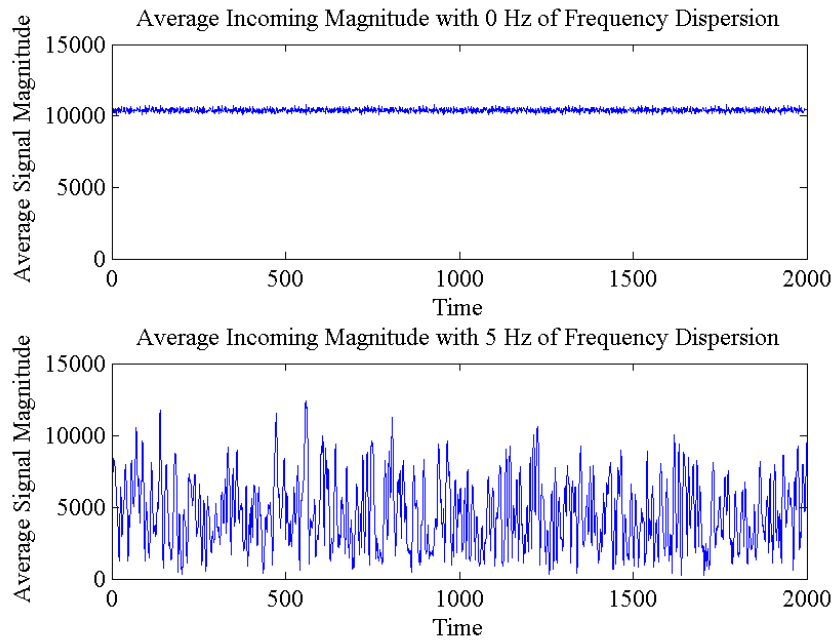


Figure 4.5 Average Incoming Magnitude with 0 and 5 Hz of Frequency Dispersion

### Receive Software Expectations

If errors are seen with frequency dispersion, there are two potential issues. One issue is the magnitude level and the other is frequency. The top image in Figure 4.6 shows the average incoming magnitude with 5 Hz of frequency dispersion. The bottom image shows when bit errors are detected at the output of the decoder.

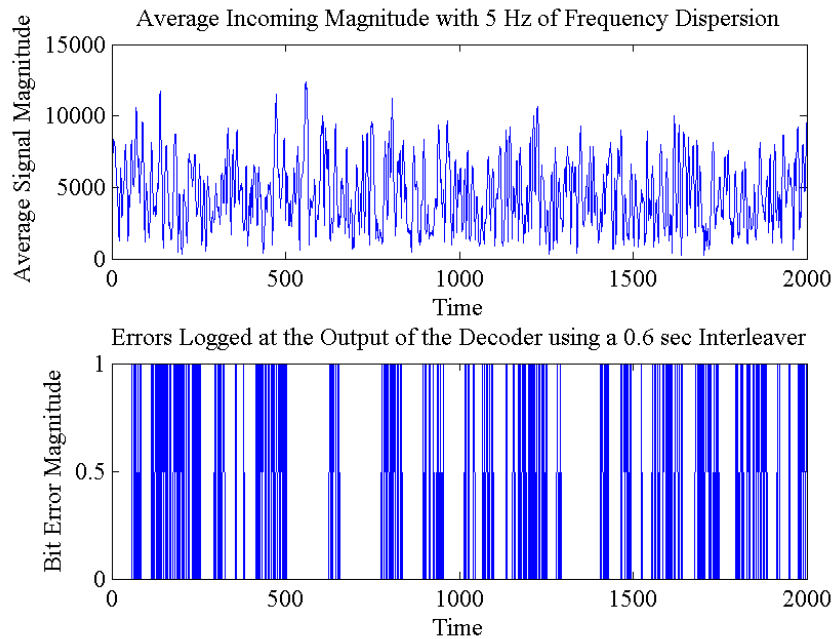


Figure 4.6 Average Incoming Magnitude and Corresponding Bit Errors with 5 Hz of Frequency Dispersion

At first glance, Figure 4.6 appears to have massive bit errors due to frequency dispersion, when the bit errors may be caused by high or low amplitude, not the frequency. To isolate the potential issue with the magnitude, begin with 0.5 msec of frequency dispersion. By setting the frequency low, errors due to the average amplitude changing rapidly should be eliminated. The top image in Figure 4.7 shows the average incoming magnitude with 0.5 Hz of frequency dispersion. The bottom image shows when bit errors are detected at the output of the decoder.

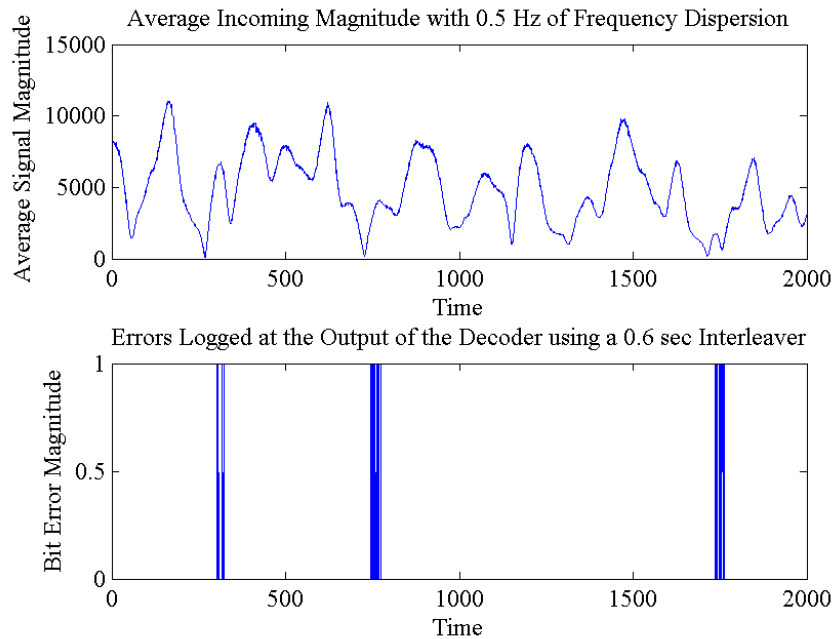


Figure 4.7 Average Incoming Magnitude and Corresponding Bit Errors with 0.5 Hz of Frequency Dispersion

The bursty bit errors seen on the bottom image in Figure 4.7 coordinate with extremely low amplitudes. Keep in mind that bit errors seen at the output of the decoder, actually correspond to the sample either 0.6 or 4.8 seconds earlier, depending on the interleaver setting. The interleaver setting used in the simulation shown in Figure 4.7 was 0.6 seconds. The delay seen between low signal magnitudes and bit errors in Figure 4.7 is directly related to the length of the interleaver, so the bit errors are due to extremely deep fades, or very low average input amplitudes.

There are two things to consider when debugging errors caused by low amplitudes from frequency dispersion. First, in bad channel environments it is assumed that a long interleaver is used. By using a long interleaver, many of the bursty errors seen in Figure 4.7 are dispersed enough for the decoder to correct them. In fact, when the same simulation shown in Figure 4.7 was run with a 4.8 second interleaver, no bit errors were seen at the output of the decoder.

Finally, time dispersion may also help eliminate some of the effects of frequency dispersion.

Having multiple paths can cause destructive interference, but may also cause constructive interference. Particularly during deep fades, the terminal relies on the constructive interference of time dispersion to boost the signal level. The errors seen with frequency dispersion may be eliminated when time dispersion is added to the channel. In order to use time dispersion to help eliminate some of the errors seen by deep fades, all software defects pertaining to time dispersion must first be eliminated.

When lower frequency dispersion rates run error free, but bit errors are seen at higher rates, the main component of interest is the internal AGC. The main purpose of the AGC is to smooth the incoming amplitude. The constellation diagram stays relatively constant in symbol amplitude when frequency dispersion is not present, creating consistent Euclidean distances for the viterbi decoder. When frequency dispersion is present and the AGC does not keep the amplitude consistent, the equalized constellation diagram appears to jitter between lower and higher symbol magnitudes, causing inconsistent Euclidean distances. Viterbi decoders do not work as well in this environment, since Euclidean distances are used to calculate metrics for soft decisions. The engineer needs to ensure that the AGC is smoothing the incoming amplitudes to allow consistent Euclidean distances for the viterbi decoder.

#### **4.2.5 Time Dispersion Isolation**

Time dispersion occurs when a signal takes multiple paths to the receiving terminal, causing multiple copies of the signal to be received with slightly different time delays. This can cause either additive or destructive interference.

##### **Simulation**

As discussed in Section 4.2.3, there are two methods to simulate time dispersion. Assuming the doppler shift and terminal clock difference issues have already been resolved, the second method using two existing radios is preferred. Most channel simulators assume that if time dispersion is present, only two paths are used. The two configurable parameters pertaining to time dispersion are delay and power. The engineer can set the amount of delay, in milliseconds, between the first and second signal. Individual power of each signal is also configurable.

Additive and destructive interference escalates when the two signals have equal power, making it the hardest power difference to recover from.

### Receive Software Expectations

Time dispersion is visible at the receive probe correlators. The top image in Figure 4.8 shows an example of a normal probe correlation. The bottom image shows a correlation with 5 msec of time dispersion.

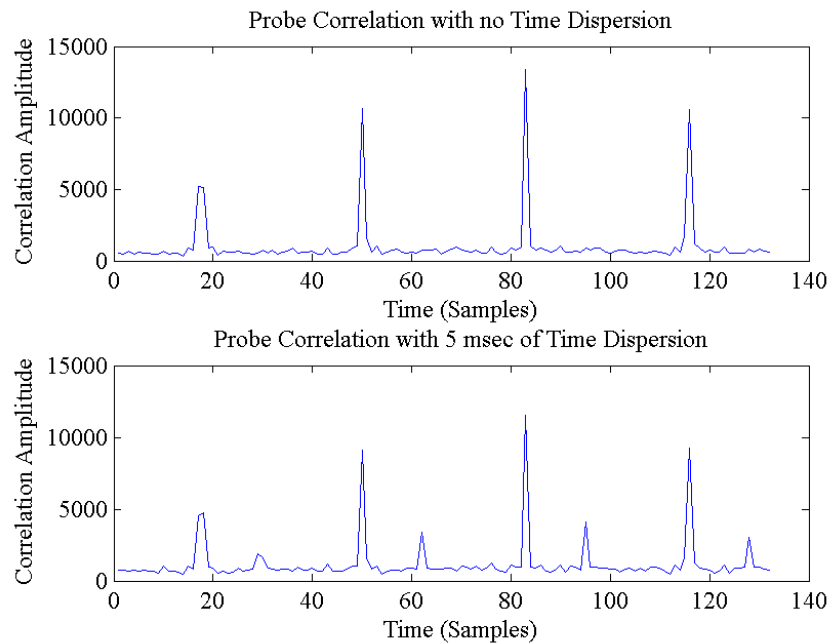


Figure 4.8 Probe Correlation with 0 msec and 5 msec of Time Dispersion

The first item to check is the delay seen within the probe correlators. Assume the incoming symbol rate to the probe correlators is 2400 symbols per second. The expected delay within the probe correlators is  $\frac{2400 \text{ symbols}}{\text{second}} \cdot 0.005 \text{ seconds} = 12 \text{ symbols}$ . It can be seen in Figure 4.8 that the smaller peak is 12 symbols from the larger peak. If the time dispersion seen in the probe correlations does not match the delay set at the channel simulator, re-check the hardware setup and the channel simulator settings.

If errors are seen with time dispersion, there are two potential issues. One issue is the delay between the two paths, and the other is the power difference. To isolate the potential issue

with delay differences, begin with a time dispersion of 2 msec and a 10 dB power difference. The top image in Figure 4.9 shows a probe correlation with 2 msec of time dispersion, while the bottom image has 5 msec.

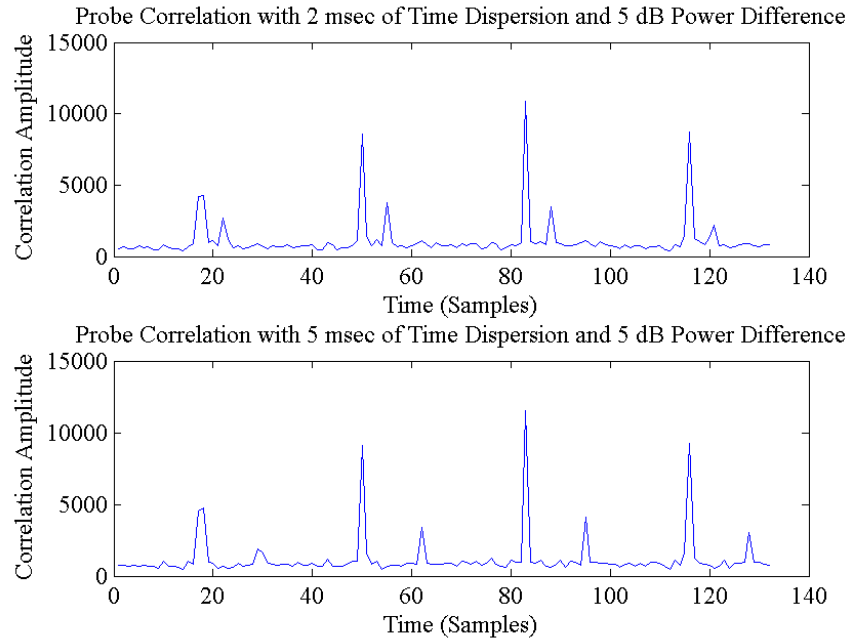


Figure 4.9 Probe Correlation with 2 msec and 5 msec of Time Dispersion

The major component on the receive data path that deals with time dispersion is the matched filter and equalizer. If the terminal logs errors with either 2 or 5 msec of time dispersion, further investigation is needed into the matched filter and equalizer. If the terminal does not log errors with 2 msec of time dispersion, but does for 5 msec, the channel estimate, matched filter, or equalizer was not designed with enough taps to correct the expected time dispersion. To compensate for 5 msec of delay the minimum number of taps used at the channel estimate is  $\frac{2400 \text{ symbols}}{\text{second}} \times 0.005 \text{ seconds} = 12 \text{ symbol taps}$ . Typically, to ensure the terminal can correct for 5 msec of time dispersion, the number of channel taps is greater than the 12 minimum. From Section 3.4.3.2, it was assumed that there were  $L + 1$  channel estimate and matched filter coefficients,  $h[n]$  and  $h^*[-n]$  respectively,  $K_2$  feedback coefficients,  $a[n]$ , and  $K_1 + 1$  feedforward coefficients,  $b[n]$ . The autocorrelation of the channel estimate was defined



as  $x[n]$  in Equation 3.4 and can be seen below.

$$x[n] = \sum_{k=0}^L h^*[-k]h[n-k]$$

Then  $q[n]$  was defined as the convolution of the feedforward filter taps and the autocorrelation of the channel estimate. It was defined in Equation 3.8 and can be seen below.

$$q[n] = \sum_{k=-K_1}^0 x[k]b[n-k]$$

For zero-forcing capability within the equalizer, it was shown that the feedforward and feedback coefficients must be assigned according to equations 3.15 and 3.14, respectively, and are shown below. It was assumed that  $K_2 \leq L$  and  $K_1 \geq L$ .

$$a[n] = q[n]$$

$$\mathbf{b} = \mathbf{X}_{simplified}^T \mathbf{q}_{simplified}$$

Where  $\mathbf{X}_{simplified}$  and  $\mathbf{q}_{simplified}$  were defined in Section 3.4.3.2 and can be seen below.

$$\mathbf{q}_{simplified} = \begin{bmatrix} q[-K_1] \\ q[-K_1 + 1] \\ \vdots \\ q[-1] \\ q[0] \end{bmatrix} = \begin{bmatrix} 0 \\ 0 \\ \vdots \\ 0 \\ 1 \end{bmatrix}, \mathbf{b} = \begin{bmatrix} b[-K_1] \\ b[-K_1 + 1] \\ \vdots \\ b[-1] \\ b[0] \end{bmatrix}$$

$$\mathbf{X}_{simplified} = \begin{bmatrix} x[0] & x[-1] & \cdots & x[-K_1 + 1] & x[-K_1] \\ x[1] & x[0] & \cdots & x[-K_1 + 2] & x[-K_1 + 1] \\ \vdots & \vdots & \ddots & \vdots & \vdots \\ x[K_1 - 1] & x[K_1 - 2] & \cdots & x[0] & x[-1] \\ x[K_1] & x[K_1 - 1] & \cdots & x[1] & x[0] \end{bmatrix}$$

To initialize these filter coefficients, it is assumed a correct channel estimate was taken. Check the channel estimate logic to be sure it matches the LMS algorithm described in Section 3.4.2.1. Mistakes can easily be made with array indices when performing signal mathematics. Be sure the correct array indices are used for  $I[n]$  and  $h[n]$  when calculating  $w[n]$  and that the correct corresponding  $d[n]$  is used to calculate  $e[n]$ . Assume  $n = 3$ rd symbol in the probe. Then,

$$w[3\text{rd symbol in the probe}] = \sum_{k=0}^L h[k]I[3\text{rd symbol in the probe} - k]$$

where  $I[3\text{rd symbol in the probe}]$  is the 3rd symbol in the known probe, and

$$e[3\text{rd symbol in the probe}] = d[3\text{rd symbol in the probe}] - w[3\text{rd symbol in the probe}]$$

where  $d[3\text{rd symbol in the probe}]$  is the received symbol believed to be the 3rd symbol in the probe based upon the preamble and probe correlations.

To isolate the other potential issue with equal power on both paths, use a time dispersion of 2 msec, but similar power. The top image in Figure 4.10 shows the probe correlation with a power difference of 5dB, while the bottom image has 0 dB power difference. Both images were created with a time dispersion of 5msec.

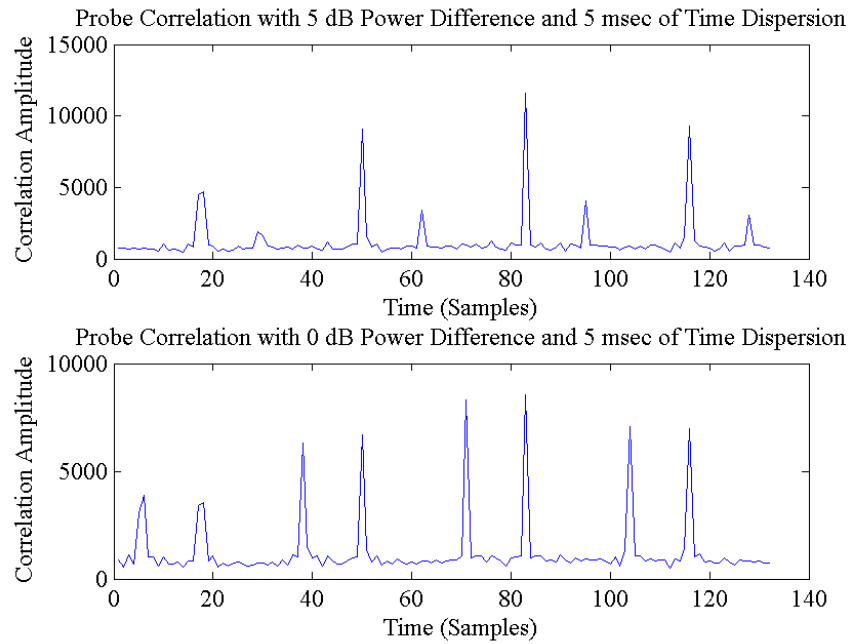


Figure 4.10 Probe Correlation with 5 dB and 0 dB Power Difference

The major components on the receive data path that address time dispersion with equal power are the probe correlator, matched filter and equalizer. If the terminal logs errors with either 2 or 5 msec of time dispersion, further investigation is needed into the matched filter and equalizer, as described earlier in this section. If errors occur only when the two paths have equal power, the component of interest is the probe correlator. The probe correlator determines which path of the two has the strongest magnitude and uses it as the major signal. As can be seen from Figure 4.10, the incoming signal has a larger magnitude on the second path. If the probe correlators choose the second path as the major signal then the remaining software should also use that same signal.

When the probe correlators, channel estimator, matched filter and equalizer are working properly, significant improvements regarding the constellation diagram can be seen. The top image in Figure 4.11 shows the unequalized constellation diagram with 2 msec of time dispersion present on the channel. The bottom image shows the improved constellation diagram after the equalizer.

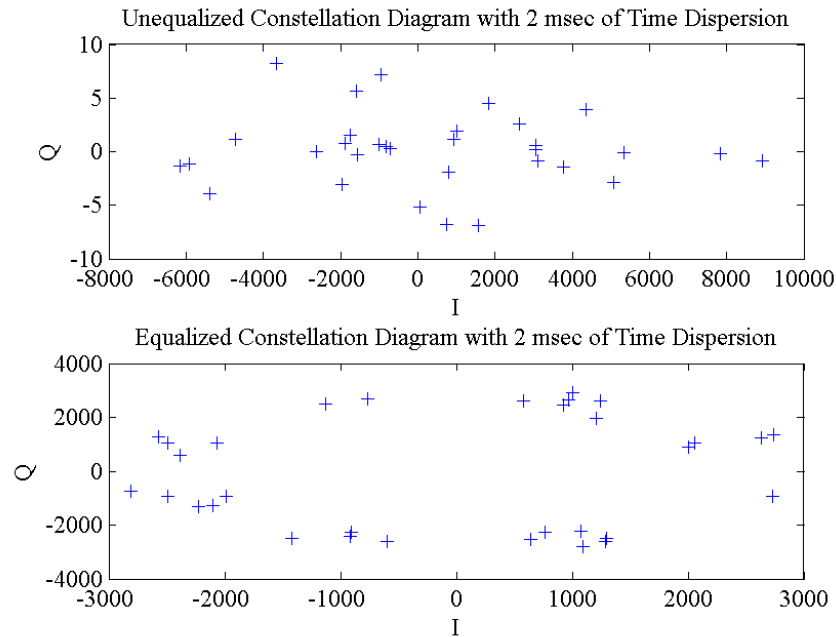


Figure 4.11 Unequalized and Equalized Constellation Diagrams with 2 msec of Time Dispersion

The equalized constellation diagram shown in the bottom image of Figure 4.11 shows the effects of the equalizer. It resembles the 8-ary PSK constellation diagram, whereas the unequalized diagram does not. As described above, time dispersion can help frequency dispersion by constructively interfering. Similarly, frequency dispersion can also help time dispersion by boosting the signal level during destructive interference. When the same simulation shown in Figure 4.11 was completed with 5 msec of time dispersion, the equalized constellation diagram hardly resembled the expected 8-ary PSK constellation. When 1 Hz of frequency dispersion was added to the 5 msec of time dispersion, the results were much cleaner. The top image in Figure 4.12 shows the unequalized constellation diagram with 5 msec of time dispersion and 1 Hz of frequency dispersion. The bottom image shows the equalized constellation.

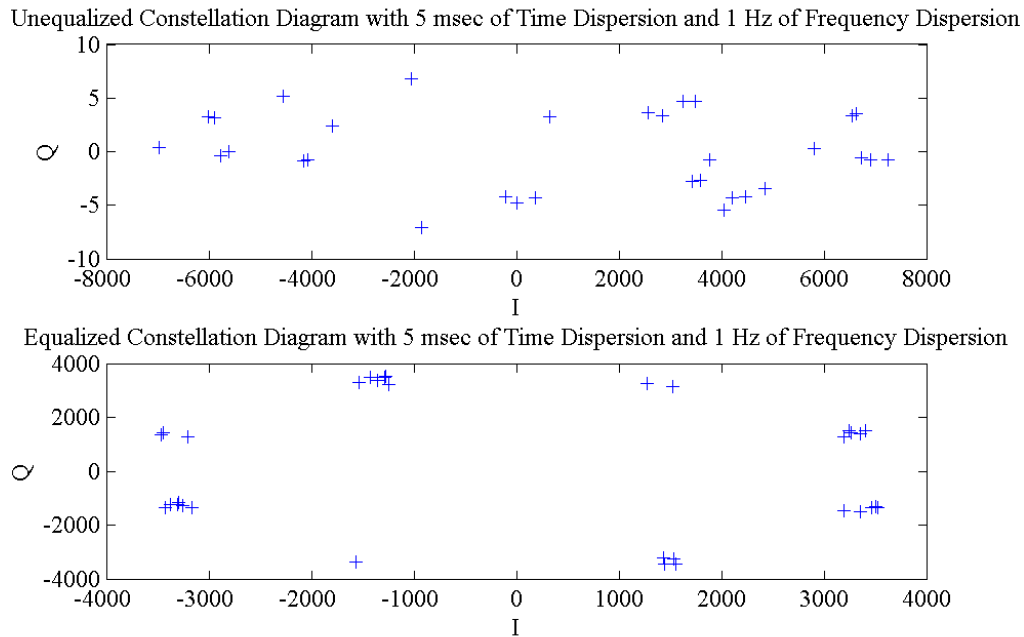


Figure 4.12 Unequalized and Equalized Constellation Diagrams with 5 msec of Time Dispersion and 1 Hz of Frequency Dispersion

By solving the software defects for frequency and time dispersion, individually, the two channel effects actually complement each other when placed on the same channel. Even though Figure 4.12 resembles the harsher channel conditions, both the unequalized and equalized constellation diagrams look cleaner than in Figure 4.11.

### 4.3 Software Isolation Summary

By using the timing of bit errors, and applying each channel effect individually, it is easier to isolate a software defect. Bit errors which occur at the beginning of a reception lead to a different area of software than errors seen at the end of reception. Likewise, the software defect which causes bit errors when frequency dispersion is applied is different that the defect which causes bit errors when time dispersion is applied. Tables 4.2 and 4.3 summarize the software isolation discussed in this chapter.

Table 4.2 Software Isolation based upon Bit Error Timing

Functionality	Beginning	End	Throughout
<b>COMMON FUNCTIONALITY</b>			
Rate Change Filter			
AGC			
Translator			
Waveshaper			
<b>PREAMBLE PATH</b>			
<b>PREAMBLE ACQUISITION MODE</b>			
Preamble Correlators			
<i>False Detection</i>	X		
<i>Initial Timing Position</i>	X		
FFT			
NSR			
<i>Initial Doppler</i>	X		X
<b>PREAMBLE TRACKING MODE</b>			
Autobaud Information Correlators			X
Preamble Count Correlators			
<i>False Detection</i>	X		
<b>END OF PREAMBLE MODE</b>			
Initialization for Data Mode			
<i>Initial Channel Estimate</i>	X		
Timing Adjustment			X
<b>DATA PATH</b>			
Probe Correlators			
Channel Estimate			
Matched Filter			
Equalizer / Demodulator			
Deinterleaver			X
Decoder			
EOM Detector		X	

Table 4.3 Software Isolation based upon Individual Channel Effects

Functionality	Doppler	Clock Dif	Noise	Freq Dis	Time Dis
<b>COMMON FUNCTIONALITY</b>					
Rate Change Filter	X				
AGC				X	
Translator	X				
Waveshaper	X				
<b>PREAMBLE PATH</b>					
<b>PREAMBLE ACQUISITION MODE</b>					
Preamble Correlators					
<i>False Detection</i>					
<i>Initial Timing Position</i>					
FFT					
NSR					
<i>Initial Doppler</i>					
<b>PREAMBLE TRACKING MODE</b>					
Autobaud Information Correlators					
Preamble Count Correlators					
<i>False Detection</i>					
<b>END OF PREAMBLE MODE</b>					
Initialization for Data Mode					
<i>Initial Channel Estimate</i>					
Timing Adjustment					
<b>DATA PATH</b>					
Probe Correlators		X			X
Channel Estimate					X
Matched Filter					X
Equalizer / Demodulator					X
Deinterleaver					
Decoder			X		
EOM Detector					

## CHAPTER 5. SUMMARY AND FUTURE WORK

This thesis provides a new HF engineer some debugging techniques for the Single Tone modem. In the future, this work can be expanded and explained in further detail. New tests and isolation techniques can be added to further expand the debugging tree. Automated testing could also be integrated with the information contained within this thesis. When the testing software logs an error, it could also log the bit error timing, and any channel effects for easier debugging. Single Tone is one of many HF modems. It would be beneficial to have similar documents for the other HF modems. While researching the architecture, it was discovered that there are many areas where better techniques could be applied. By writing this type of document, each section of software can be looked at in detail and determine if better implementation techniques are available.

The MIL-STD-188-110A Single Tone high frequency modem is used by the United States military as a beyond line-of-sight radio which uses the ionosphere for reflection, rather than a satellite. The HF Single Tone modem needs to account for typical channel effects such as doppler shift, terminal clock differences, and noise in addition to some channel effects caused by the ionosphere such as frequency and time dispersion. The signal processing software can be difficult to debug when failures occur during performance testing. This thesis provides a method of debugging by concentrating on two major steps: understanding and isolation. The engineer must understand the channel model and receive path in order to correlate a test failure with a specific section of software. This thesis provides a description of both the channel model and receive path. After the channel model and receive path are understood, isolation of a test failure through timing patterns of bit errors and individual channel effects help the engineer isolate the software defect. This thesis creates a matrix of test failures with software isolation



of which to use for debugging.

## APPENDIX ACRONYNS

AM	-	amplitude modulation
AGC	-	automatic gain control
ADC	-	analog to digital converter
AWGN	-	additive white gaussian noise
BER	-	bit error rate
bps	-	bits per second
CW	-	continuous wave
DAC	-	digital to analog converter
DFE	-	decision feedback equalizer
DSB	-	double side band
EOM	-	end of message
FEC	-	forward error correction
FFT	-	fast fourier transform
FPGA	-	field-programmable gate array
FSK	-	frequency shift keying
HF	-	high frequency
IF	-	intermediate frequency
ISI	-	inter-symbol interference
LMS	-	least mean square
LOS	-	line-of-sight
LSB	-	lower side band

NSR	-	noise to signal ratio
PSK	-	phase shift keying
RF	-	radio frequency
SNR	-	signal-to-noise ratio
sps	-	samples per second
SSB	-	single side band
USB	-	upper side band
ZF-DFE	-	zero-forcing decision feedback equalizer

## BIBLIOGRAPHY

- [1] John W. Neito, *On-Air results of Spatial Diversity for the MIL-STD-188-110B Appendix C (STANAG 4539) 9600 bps waveform*, IEEE 2001, pp. 432–436
- [2] Collins Defense Communications, Publ. 523-0767157-002217, HF Communications Data Book, June 1978
- [3] MIL-STD-188-110A, *Mil. Std. Interoperability and Performance Standards for Data Modems*, US Dept of Defense, September 1991
- [4] MIL-STD-188-110B, *Mil. Std. Interoperability and Performance Standards for Data Modems*, US Dept of Defense, March 1999
- [5] J. Proakis, *Digital Communication*, McGraw Hill, ISBN 0-07-232111-3, 4th Edition
- [6] W. N. Furman and J. W. Nieto *Understanding HF Channel Simulator Requirements in order to Reduce HF Modem Performance Measurement Variability*
- [7] *Equations for the Raised Cosine and Square-Root Raised Cosine Shapes* Brigham Young University Department of Electrical and Computer Engineering 25 October 2008  
<http://www.ee.byu.edu/class/ee485public/ee485.fall.99/lectures/raised-cosine.pdf>

## ACKNOWLEDGEMENTS

I would like to take this opportunity to express my thanks to those who helped me conduct my research. Thank you to Dr. Zhengdao Wang for his guidance, patience and support throughout this process. To my other committee members, Dr. Robert Weber and Dr. Aleksandar Dogandzic, thank you for agreeing to serve on my committee. Thanks to Pam Myers for all of her help. Also, thanks to the entire DSP team at Rockwell Collins for their expertise.